This is the accepted manuscript version of the contribution published as:

Ma, X., Du, Y., Peng, W., Zhang, S., Liu, X., Wang, S., Yuan, S., **Kolditz, O.** (2021): Modeling the impacts of plants and internal organic carbon on remediation performance in the integrated vertical flow constructed wetland
Water Res. **204** , art. 117635

The publisher's version is available at:

http://dx.doi.org/10.1016/j.watres.2021.117635

Modeling the plant effects of aeration and organic exudates on remediation performance of an integrated vertical constructed wetlands

Xiaoyu Ma [1], Yanliang Du [1], * Wenqi Peng[1], Shuanghu Zhang[1], Shiyang Wang[1], Shoujun Yuan[2], Chang Liu[1], Olaf Kolditz[3]

[1] China Institute of Water Resources and Hydropower Research (IWHR), China

[2] Department of Municipal Engineering, School of Civil Engineering, Hefei University of Technology, Hefei 230009, China. sjyuan@hfut.edu.cn

[3] Department of Environmental Informatics, Helmholtz Centre for Environmental Research, UFZ, Leipzig, Germany

***** Correspondence: duyl@iwhr.com; Tel.: +86-15210429872

Received: date; Accepted: date; Published: date

Abstract: The integrated vertical constructed wetland (IVCW) consists of two or more chambers with heterogeneous flow patterns and strong aeration capability, possesses favorable remediation performance. The Constructed Wetland Model No.1 (CWM1) coupled with the OpenGeoSys # IPHREEQC was applied to investigate the wetland plant effects on treatment efficiency. Considering two fundamental functions of the plants, (i) the oxygen release as radial oxygen loss (ROL) and (ii) exudation of internal organic carbon (IOC) from roots are developed and implemented in the numerical model to simulate the treating processes of two parallel laboratory-scale IVCWs fed by artificial wastewater with and without plant. The good agreement between simulated results and measurements of planted and unplanted IVCWs demonstrate the combined effects of ROL and IOC of the

plants and the model reliability. In summer the ammonia (NH_4-N) and total nitrogen (TN) removals are high as above 90% in both IVCWs, and in winter they decline significantly to around 55% and 45% in unplanted CW, contrastively to about 85% and 78% in planted CW. According to the model simulation, for high TN removal of no-planted and planted IVCWs, the COD/N ratios are about 3-7 and 3-10 gCOD/gN, which can be utilized to evaluate organic carbon loading status. The ROL in the unplanted CW promotes COD and NH_4-N removal, while may inhibit the denitrification under low temperature condition. Single addition of IOC enhances the oxygen consuming and restrains the nitrification, because of the full loaded COD. Summarized the organic carbon released from substrate and roots as total IOC, the quantification of IOC acts on nitrogen treatment were simulated and compared with the external organic carbon (EOC) loading from influent. At same organic loading rates, IOC performs higher efficiency on TN removal than EOC. The results provides the thoughts of the solution for low TN removal in constructed wetlands.

Keywords: *Integrated vertical constructed wetland (IVCW); CWs modeling; Plant effects; radial oxygen loss (ROL); Internal organic carbon (IOC); COD/N ratio; Total nitrogen removal;*

1. Introduction

Constructed wetlands (CW) are engineering systems designed and assembled with economical advantage in lower operational and maintenance costs to treat wastewater in a more controllable conditions. Plants are regarded as an essential component of CWs, that the stem and leaf above the substrate play the role of landscaping ornament, recreation, wildlife habitat creation, alleviating the influence of cool and hot weather, as well as the nutrient removal capacity (Wang et al. 2017, Hua et al. 2018). CWs with plants were observed

having more stable treatment performance and higher removals, especially for nitrogen rather than BOD and COD, comparing with no plants CWs (Tanner 2001, Huett et al. 2005, Zhu et al. 2014, Pelissari et al. 2016, Teixeira et al. 2018, Carrasco-Acosta et al. 2019).

The contribution of plants to the treatment performance has been widely discussed. The primary perception of nutrient removal pathway by plants in CWs was the nutrients uptake. Ammonium is the preferential biotic uptake source among inorganic nitrogen (Nayar et al. 2010). Comparing to the loadings from wastewater, the amount of nutrients removed by plant harvesting is generally insignificant (Brix 1997, Bachand 2000, Kim 2001). The proportion of nitrogen removal by plants uptake in CWs are 4–11% and 2–8% given by Lin et al.(2002) and Tanner (2001), respectively, while nitrogen removal due to denitrification were about 89–96%(Lin 2002). As for low loaded systems, especially for the horizontal subsurface flow CWs, the amount of nutrients removed by plants can be high (Greenway 2001, Kyambadde et al. 2004). The nutrients incorporated in the un-harvested plants return to the CW system during decomposition. The expected maximum nitrogen and phosphorus removal by plant uptake directly and harvesting are small (Yang 2001, Lin 2002, USEPA 2011), which was neglected in some modelling research (Giraldi et al. 2010).

Going deep to the plant roots in the CWs substrate formed rhizosphere zone is the habitat of an overwhelming number of microorganisms and invertebrates and is considered to be one of the most dynamic interfaces on Earth (Philippot et al. 2013). Plants roots can accelerate the development of microbial communities by promoting alternate aerobic and anaerobic micro-environments (Stottmeister et al. 2003). Internal aeration is crucial for root growth under anoxic conditions, and the oxygen transported via the aerenchyma to the root tips, enabling root growth into anoxic soil(Haichar et al. 2008). The oxygen release to the soil called radial oxygen loss (ROL) were observed and measured, and quantified. Significant differences among species were tested, ROL in the rhizosphere have been positively correlated (35~76%) with the removal of TN among differences plant species

(Mei et al. 2014). Generally, ROL was positively correlated with photosynthetic rate, transpiration rate, root activity, root biomass, above-ground biomass, leaf biomass, root porosity, maximum root length, and removal rates of TN and TP (Lai et al. 2012). The addition of biochar in CWs also can improves the ROL(Hang et al. 2019). The oxygen profiles patterns in rhizosphere present oxygen saturation peaked around the middle part of roots and the thickness of stably oxidized zones increased as the roots grew(Wang Wenlin et al. 2014). The oxygen transport model between root and soil were studied and established (Cook and Knight 2003, Cook et al. 2013).

Plant roots may release up to 20% of their photosynthesis products into soil, providing the basis for the establishment of plant–microorganism interactions (Haichar et al. 2008) The newly generated carbon derived from root exudates, and ancient carbon in soil organic matter, are available for microbial growth (Caspersen 2004, Wu 2012). The majority of root exudates including primary metabolites (sugars, amino acids, and organic acids) are regarded to be passively lost from the root and used by rhizosphere-dwelling microbes (Dundek et al. 2011, Canarini et al. 2019). The plants shows high power on organic matter degradation through bacteria caused by root exudation. Moreover, wetland plants deliver organic carbon via root exudates to fuel the microbial denitrification process in constructed wetland systems receiving nitrate-rich and low-carbon wastewater. Zhai et al. (2013) shows DOC release rates from root amounted to 0.6–4.8% of the net photosynthetically fixed carbon. Extrapolating the laboratory measurements to field conditions suggests that plant root exudates may potentially fuel a denitrification rate of 94–267 kgN ha^{-1} $year^{-1}$ in subsurface flow constructed wetlands. Root exudates are potentially important as an organic C source for denitrification in lightly loaded subsurface flow constructed wetland. Root exudates can act as endogenous carbon sources for heterotrophic denitrifying bacteria and ultimately determine the microbe distribution patterns in micro-polluted CWs(Wu et al.

2017). Nutrient removal was positively correlated with microbe density in rhizosphere which affected by root exudates (Chen et al. 2016).

The denitrifying bacteria require labile organic carbon (C) as an energy source denitrification (Clement 2002). The organic loading rate (OLR) influents the nitrifying and denitrifying bacterial community (Pelissari et al. 2016), the excessive and insufficient organic carbon lead to the reduction of nitrogen removal (Ding et al. 2012, Wu et al. 2013). In the numerous practices of wetland construction and operation in China, the treat performances were usually restricted by low COD/N ratios (Xie et al. 2012, Zhang et al. 2012). In order to promote the CWs removal, although numerous researches focused on the COD/N ratios of influent wastewater (Ding et al. 2012, Akizuki et al. 2015, Wu et al. 2017, Wang et al. 2020). The planted CWs achieve efficient nitrogen removal under the both high and low COD/N conditions (Huett et al. 2005, Zhu et al. 2014). It is difficult to set a guideline value on COD/N ratio for high nitrogen removals, which are related to wetland configurations, operation mode, plantation, nitrogen composition and types of wastewater to be treated (Saeed and Sun 2012). Nevertheless for the certain CWs, the COD/N ratios can be the guidance to evaluate whether the CW is overloaded or light loaded by COD.

The properties of substrates predominate not only the hydrodynamics but also the biological dynamics, adsorption and fixation process, consequently influence the treatment efficiency (Wang et al. 2017, Lima MX 2018, Shi et al. 2018, Xu et al. 2019). The concept of internal supplies of organic carbon from the filler was brought out as an alternative solution by Saeed and Sun (Saeed 2011a, 2011b), and Tee et al. (2012). The background concentration in substrates in terms of organic carbon is often assumed to be around 3 mg L^{-1} (Rousseau et al. 2004). The impacts of some different unconventional substrates on the nitrogen and organics removal were summarized (Saeed and Sun 2012). Some fillers were selected for internal organic carbon (IOC) supplement, which can promote denitrification and improved nitrogen treat performance (Saeed and Sun 2017, Wang et al. 2017, Xu et al.

2019). It should be mentioned that the additional IOC may only benefits the micro-pollutant water and deficient carbon system. Most researches provided the options of filler selection for better treatment. It is difficult to assess the effects of quantitative IOC loading as well as spatial assembly of IOC on the removal by experiments.

Constructed wetland (CW) models have been considered as an important tool to enhance understanding of the simultaneous physic-chemical and biological processes, and to optimize the design and operation of CWs. In general the process-based models consist of hydraulic module, transport module, biochemical module. Most biochemical module were developed based on Activated Sludge Models (ASM) to simulate the biokinetic process. Recent years, the improved CWM1 become popular for modelling (Langergraber et al. 2009, Boog et al. 2019, John et al. 2020). Based on the framework of CWs model, some mechanistic processes were implemented in the model to investigate combined effects caused by external and internal factors. The clogging process (Giraldi et al. 2010, Rajabzadeh et al. 2015, Boano et al. 2018), aeration and temperature impacts(Boog et al. 2019, John et al. 2020), plants effects (Samsó and Garcia 2013a) were successfully modelled.

The present study is based on observation results from two laboratory-scale experimental constructed wetlands (IVCW), which were filled with zeolite, one was planted with Phragmites australis and the other was unplanted. The radial oxygen loss (ROL) and internal organic carbon (IOC) exuded from plants roots, associated with the adsorption, clogging effects, are developed and implemented in biological dynamics model of CWM1, which is coupled to a reactive transport model OpenGeoSys#IPHREEQC. The comparison between the experimental measurements and modelling results are carried out in order to calibrate the parameters and verify the reliability of the model. The appropriate COD/N ratios for efficient nitrogen removal in unplanted CW and planted CW are calculated by model instead of conventional experiments, consequently the carbon loading levels can be

evaluated by the obtained ratios. As the important factors, ROL and IOC are simulated, respectively, for a whole year to analyze the seasonal treatments alteration along with the bacteria activities and temperature changes. For deficient carbon system, many experiments focused on the filler selections, and the quantitative supplements of IOC and its impacts were difficult to assess. Following the concept of internal carbon source, the model calculates the nitrogen removal variation with the growth of external organic carbon (EOC) and the internal organic carbon (IOC) respectively, to the further understanding on the spatial function of carbon sources.

The paper is structured as follows: the section of "Materials and methods" introduces the design and operations of the experimental planted and unplanted IVCWs, as well as the descriptions and settings for two IVCWs in the numerical model; the section of "Results and discussion" presents the verification of the planted and unplanted IVCWs modelling, and some discussions on the impacts of hydrodynamics, COD/N ratios, temperature and the internal carbon sources. Finally, the results and discoveries are summarized in the "Conclusions" section.

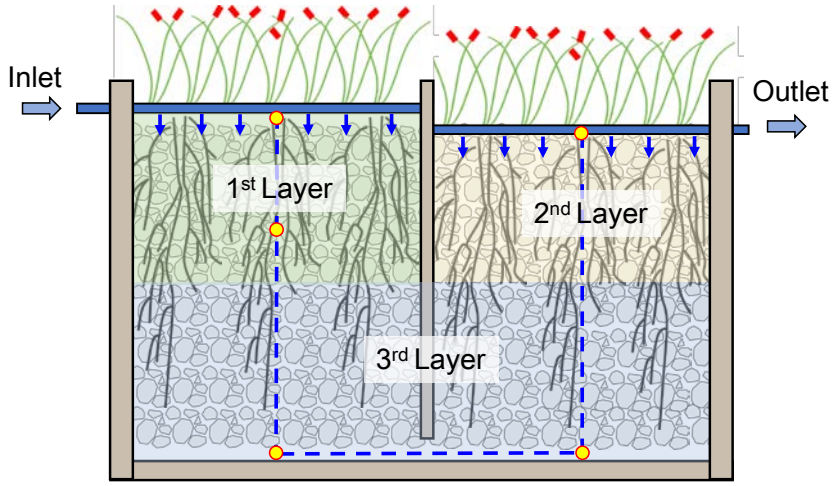
2. Materials and Methods

2.1 Experimental IVCW

Taking the advantage of horizontal subsurface-flow CWs and vertical subsurface-flow CWs, the integrated vertical-flow constructed wetland (IVCW) with relatively high treatment performance for common pollutants has become one of the main CW types in China (Chen et al. 2008, Chang et al. 2013). The experimental scale IVCWs with internal measured data were elected for our work.

The laboratory-scale experiments were carried out in Hefei University of Technology. There were several IVCWs with identify size, which were 1m long, 0.5m wide and 0.65m height, with a bottom slope of 0.5%. Each IVCW was divided into a down-flow chamber

176 (DFC) and an up-flow chamber (UFC) by a vertical clapboard in the middle, which left
177 10mm a narrow slit at bottom for the connection of chambers (Fig 1). The surface
178 elevations of down-flow chamber were 100mm higher than those of the up-flow chamber.
179 The water pipes were distributed on the surface of the down-flow chamber, and water was
180 gathered on the surface of the up-flow chamber.



181

182 **Fig. 1.** Schematic diagram of experimental design and setting

183 The experiments were designed to study the effects of wetland plants. There were two
184 parallel IVCWs filled by granular zeolite, as one with plants and the other without plant.
185 The granular media consisted of two layers, bottom layer was 0.3m thick composed of
186 coarser gravels (D = 4~8 mm, initial porosity n = 45%), and up layer was 0.35m thick with
187 fine gravels (D = 2~4 mm, initial porosity n = 40~45%). The Phragmites australis were
188 transplanted in IVCWs in March 2014, and grew well in the summer. The wetland plants
189 started to wither in Oct and were harvested in Dec. The IVCWs in summer and winter are
190 shown in Fig. 2. The monitoring was carried out after several months till its stable operation
191 in June 2014.



Fig. 2. Experimental IVCWs in summer and in winter

192

193 Although the model can calculate the spatiotemporal variations of water components in
194 the wetland, many experiments usually provide the changes between influent and effluent,
195 and the internal alterations are mostly similar to the “black box”. To investigate the water
196 variation inside the IVCWs, there were 3 internal sites along the flow stream for sampling,
197 which were shown in Fig 1. During the feeding period, the wetland were operated with
198 hydraulic loading rates (HLR) of approximately 0.24 m^3d^{-1} and hydraulic retention time
199 (HRT) of 2.7 days. The intermittent artificial wastewater supplies are fed to IVCWs, and the
200 influent concentrations of components as organic loading (glucose), NH_4-N, TN and DO
201 were shown in Table 1. The total nitrogen in influent mainly consists of ammonia in
202 experiment, and with COD/N ratio is around 5.9~7.1.

203

204 **Table 1.** Influent concentrations of each component

	COD	TN	NH_4-N	DO	pH
	$mg•L^{-1}$	$mg•L^{-1}$	$mg•L^{-1}$	$mg•L^{-1}$	
Influent	47.56-54.11	7.66-8.81	6.21-8.18	2.4-4.9	6.14-7.44

205

206 ***2.2 Model description***

207 *2.2.1 Model setup*

208 The established model framework OGS# IPHREEQC coupled with Constructed
209 Wetland Model No1 (CWM1) has been applied for IVCWs modelling in this study.
210 OpenGeoSys (OGS) is an open source finite element simulator for
211 thermo-hydro-mechanical-chemical processes which has been developed over more two
212 decades (Kolditz et al. 2012, Bilke et al. 2019). OGS has been used in various
213 environmental disciplines such as water resources management, soil physics, geothermal
214 energy systems and deep geological deposition of hazardous waste. In the present work the
215 capabilities of OGS for multicomponent transport processes in variably saturated porous
216 media are used (Kalbacher 2011). PHREEQC is one of the most widely used open-source
217 geochemical solvers for aqueous, mineral, gas, surface, ion exchange, solid-solution
218 equilibria and kinetic reactions, it can also provide a well-defined set of methods for data
219 transfer and management (Charlton and Parkhurst 2011). CWM1 is a general model to
220 describe biochemical transformation and degradation processes for organic matter, nitrogen
221 and sulphur in subsurface flow constructed wetlands, which can be appended in the
222 framework of PHREEQC. Since both OGS and PHREEQC are open-source model, they
223 have been technically coupled on the code level as OGS# IPHREEQC (“I” stands for
224 “interface”) (He et al. 2015, Lu 2017).

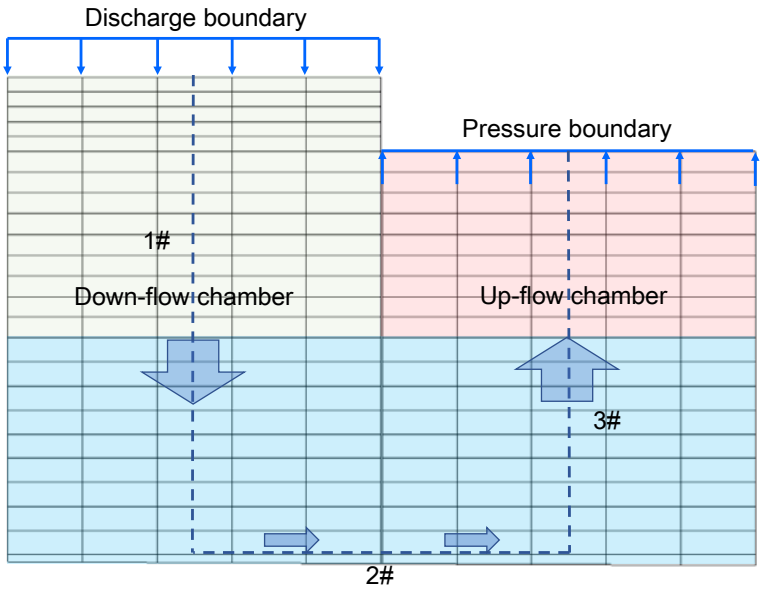
225 The IVCWs has two chambers results spatial heterogeneous distribution of
226 hydrodynamic and water quality components. The computed domain is discretized by

quadrangle meshes, and divided into 3 sub-domains filled with 3 different porous material, which is shown in Fig. 3.

The influent and effluent boundary conditions of hydrodynamics and water quality are set up on the surface of the down-flow chamber and the up-flow chamber respectively. The inflow rates, and concentration of COD, NH_4-N, and TN are identify for both IVCWs. The influent water is well distributed on the down-flow chamber surface, with the hydraulic loading rate as 0.24 m/d. The time series of COD, NH_4-N and TN concentration are from the measurements. Since the COD of inflow is made by glucose in the experiment, the influent COD is regarded as biodegradable dissolved COD (S_F) in the model, and the easily biodegradable particle COD (X_S) is 0.

The measured influent concentrations of components as organic loading (glucose), NH_4-N, TN and DO associated with discharges were input as discharge boundary. The outflow boundary is set as pressure boundary with zero gradient concentration. Initially, all water quality variables including bacterial components are set to zero in computed domain. In the planted IVC, the two chambers are almost full-filled by the roots of well-grown Phragmites australis, which are set as root zones in modelling. Although the reeds were harvested in winter, the functions of roots are still active.

The computation domain, meshes and boundary conditions in the model are indicated in Fig. 3.



246

247 **Fig. 3.** Computation domain, meshes, boundary and defined output polyline.

248 In order to investigate the spatial variations in IVCW, 1 polyline is defined for the
249 model output, also shown in Figure 2. The polyline starts from the surface of down-flow
250 chamber down to the bottom (line1#), then go to the horizontal direction at bottom to
251 up-flow chamber (line 2#), finally it from the bottom to the surface of UFC (line 3#).

252 *2.2.2 Hydraulic module*

253 The unsaturated and saturated zone both exist in the IVCWs, the Richards equation is
254 used to describe the water flow through porous media (Kolditz et al. 2015):

$$-n\rho_w \frac{\partial \theta}{\partial p_c}\frac{\partial p}{\partial t} - \nabla \cdot \left[\rho_w \frac{\mathbf{k}\kappa_{rel}}{\mu}(\nabla p - \rho_w g)\right] = Q_w \quad (1)$$

255 where n represents the porosity, -; Sstands for the saturation, p and p_c mean pressure
256 and capillary pressure, respectively, Pa; $\rho_w$is the water density, kgm^{-3}; μ is the viscosity,
257 kg m^{-1} s^{-1}; κ_{rel} is the relative permeability, m^2; **k** is the intrinsic permeability tensor, and
258 Q_w is the source/sink term, m^3 s^{-1}.

259 The constitutive relationships between pressure, saturation, and hydraulic conductivity
260 use van Genuchten model and the related empirical parameters for unsaturated conditions:

$$p_c = \rho_w g \left[\theta_{seff}^{-\frac{1}{1-(1/m)}} - 1 \right]^{\frac{1}{m}} \quad (2)$$

$$\theta_{seff} = \frac{\theta - \theta_s}{\theta_s - \theta_r} \quad (3)$$

Where, θ_{seff} is effective saturation, θ_r and θ_s are the residual and saturated volumetric water content, m is coefficient in van-Genuchten model.

2.2.3 Biological dynamic model

Biological dynamic module is used constructed wetland model CWM1 (Langergraber et al. 2009), which models the dissolved oxygen, organic carbon, organic nitrogen, ammonia and oxidized nitrogen, hydrogen sulphide and sulfate, as well as the growth and decay of heterotrophic, fermenting, autotrophic, methanogenic and sulfate reducing and sulphide oxidizing bacteria. CWM1 computes 17 processes and 16 components. The computed component consists of 8 dissolved species and 8 particulate species. Dissolved species, indicated by Si (i=1, 2, …), are only present in the aqueous phase, and particulate species, indicated by Xi (i=1, 2, …), are defined both in the aqueous (mobile) and solid (immobile) phases. Part of the COD and all bacteria species belong to the particulate species. The particulate components participate the attachment and detachment processes, and transform between mobile and immobile statues.

The transport of aqueous (mobile) components with absorption effects in unsaturated porous media is described by equation (4) as:

$$n\frac{\partial \theta C_i}{\partial t} + \rho_s \frac{\partial S_{ads}}{\partial t} = n\nabla\theta(\mathbf{D}\nabla C_i - qC_i) + Q_{Ci} + r_{Ci} \quad (4)$$

Where i=1,2,…k, k is the total number of aqueous phase species (dissolved and particulate), C_i is the aqueous phase concentration of the i^{th} species. S_{ads} is adsorbed concentration, kg kg^{-1}; ρ_s is density of substrate, kgm^{-3}; D is the hydrodynamic dispersion

283 tensor, m^2 d^{-1}; q is the Darcy velocity, m d^{-1}; Q_{Ci} represents the source/sink term of C_i,
284 $mgL^{-1}d^{-1}$ and r_i denotes the reaction rate of C_i, $mgL^{-1}d^{-1}$.

285

286 **(1) Aeration**

287 Dissolved oxygen is an important component to influence the treatment performance of
288 IVCW. The porosity of the unsaturated zone bring air into substrates, and intermittent water
289 supply generating saturation changes is used for aeration. Oxygen transfer rate (OTR) from
290 air to water is the function of properties, temperature, concentration of saturated dissolved
291 oxygen and local dissolved oxygen. GarcÍA et al (2010). pointed out that the oxygen
292 transfer coefficient is an inverse proportion function of depth especially in vertical flow
293 CWs. Combining the depth impacts on OTR, we developed the equation (5) to calculate the
294 OTR.

$$\mathrm{OTR} = (k_{La,T,A} * \theta + k_{La,T,R} * (1 - \frac{z}{z_{max}}))(S_o^* - S_o) \quad (5)$$

295 Which $k_{La,T,A}$ is the oxygen transportation coefficient of surface reaeration; $k_{La,T,R}$
296 is t Coefficient in Oxygen transmission rate of intermittent water supply; z is the depth;
297 z_{max} is the maximum depth; S_o^* is saturated dissolved oxygen, mg L^{-1}; S_o is the dissolved
298 oxygen, mg L^{-1}.

299 Additionally, the radial oxygen loss (ROL) of the plant root also named oxygen release
300 is counted in the aeration sources. The oxygen release rate were about 0.45 ~5 (gO_2 m^{-2} d^{-1})
301 set as constants or given curves in previous modelling (Langergraber and Šimůnek 2012,
302 Mburu et al. 2012, Samsó and Garcia 2013b). Photosynthesis of plants increases oxygen
303 partial pressure in the blades, and help O_2 transport to the underground parts through
304 aerenchyma, and spread O_2 to the rhizosphere in the form of ROL. In winter although the
305 leaves wither in winter, the reservation of ventilation tissue promotes the ROL. In this study,

306 ROL is referred to the formula from Cook et al .(Cook and Knight 2003, Cook et al. 2013),
307 is calculated by Equation (6).

$$\mathrm{ROL} = \frac{2\pi D_l L_0 (S^*_{root} - \alpha_o S_o)}{\ln(R/a)} \exp(-z/Z_r) \quad (6)$$

308 Where D_l is the diffusion coefficient for oxygen in the soil water [m^2s^{-1}]; L_0 is the
309 root length density at z=0, mm-3; $S^*_{root}$is the interface between the saturated soil layer and
310 root surface in the liquid phase, mgL-1; z is the depth, m; Z_r is the scaling depth, m; R
311 is the radius of a zone of saturated soil around the root plus the root, m ; a is the
312 parameters of the root radius, m. Depth is the main factor effect the magnitude of ROL, the
313 ROL is high in surface layer and decreases exponentially against the depth.
314

315 **(2) Internal organic carbon (IOC) loading from root exudate.**

316 The organic loading changes the microbial community and determines the growth of
317 heterogeneous denitrifying bacteria (Zhai et al. 2013). In aerobic environment, organic
318 matter can be metabolized by a large number of heterotrophic bacteria through oxygen. The
319 internal organic loading from filling material and root exudates should not be ignored. As
320 for the gravels without specially treated, the plants roots are the largest internal source of
321 organic matter. According to the experimental researches, DOC released by root is affected
322 by photosynthesis, temperature, light-regime, nutrient availability and the plant species
323 (Van Veen 1991). Carbon released from living plant roots to soil have been reported to
324 account for 15–25% of below-ground allocated carbon (Kuzyakov 2002) and 10–40% of
325 the net primary production of the plants (Warembourg 2003). In daytime or high
326 temperature roots exudes more organic matter than in the dark or low temperature. In this

study, considering the temperature impacts on plant roots, we introduce the internal organic carbon (IOC) loading by plants as：

$$\mathrm{IOC} = K_{\mathrm{root}} \cdot \theta_{rc}^{(T-20)} \quad (7)$$

in which, K_{root} is the organic carbon exudate from plant roots at 20℃, $mgL^{-1}\,h^{-1}$. θ_{rc} is the temperature coefficient. T is the water temperature. The IOC from roots is assumed as the uniform distribution in computed domain.

(3) Ammonia absorption

The zeolite is common for the substrates in wetland therefor was selected in this experiment. The zeolite is an adsorbent with strong adsorption capacity because of the powerful cation exchange capacity (Collison 2014), The ammonium was adsorbed by substrate besides conversion into nitrates during feeding period, and the adsorbed mass of ammonium was nitrified during the rest period provoking high nitrates concentrations consequently (Morvannou et al. 2014) . The adsorption capacity of zeolite were calculate by Langmuir isothermal adsorption equation described by Equation (8).

$$S = \frac{S_{max} K_{\mathrm{L}} C}{1 + K_{\mathrm{L}} C} \quad (8)$$

where, S is the amount of adsorbate on the adsorbent, $g \cdot g^{-1}$; K_{L} means the distribution coefficient of Langmuir, $m^3 g^{-1}$; S_{max} is the maximum amount of adsorbate on the adsorbent, $g \cdot g^{-1}$; C is the concentration of the dissolved species, $g\ L^{-1}$. The coefficient values of S_{max}, K_L refer to the experimental studies (Lu et al. 2016).

(4) Clogging and limitation of biomass

347 The clogging process led by the particle materials attachment on the substrate is
348 considered in the simulation following by (Samsó and Garcia 2013b, Boog et al. 2019). The
349 particle COD composed of X_S and X_I, which are both separated to the mobile and immobile
350 parts, obeys the 1st-order attach-detach process.

351 Additionally, the processes are taken into consideration referring Boog, (2019) and
352 Samsó (2013): (1) Microbial reproduction over the medium impedes bacterial growth, the
353 parameter is M_{bio_max}; (2) Restriction of bacterial growth by particulate matter attached to
354 the medium, the parameter is M_{cap} (Equation 9).

$$\frac{\partial X_i}{\partial t} = K_{grow}\left(1 - \frac{\sum X_k}{M_{bio_max}}\right)\left(1 - \frac{X_I}{M_{cap}}\right)X_i - K_x \quad (9)$$

355 in which, X_i is the concentration i[th] bacteria, ngL-1; K_{grow} is the maximum growth rate of
356 bacteria, mg L^{-1} h^{-1}; M_{bio_max} is the concentration of total microbial species which arise the
357 microbial reproduction growth limitation, g L^{-1}; M_{cap} is the concentration of total particle
358 maters which limit the growth of microbial matters, g L^{-1}; X_I is the inert particle COD. K_x is
359 the hydrolysis rate of bacteria, mg L^{-1} h^{-1}.

360 ## *3. Results and Discussion*

361 ### *3.1 Model calibration*

362 The IVCWs with plant and without plant are modelled by CWM1. The modelled time
363 period are consistent with experimental period from May 2014 to Aug 2015. The influent
364 concentrations of components as organic loading (glucose), NH_4-N, TN and DO were
365 measure frequently, shown in Table 1. These concentrations correspond to mean values
366 measured in all samples and are 0 for S_{NO}, S_{H2S}, and S_{SO4}. Influent concentrations of bacteria

groups are generally very small in comparison to the amount present within the granular media and were neglected.

The influent COD consisted of inert COD (CI), readily biodegradable COD (CR) and slowly biodegradable soluble COD (CS). The fractioning of the influent COD was made using recommended values for primary effluents in Activated Sludge Models (ASMs) (Henze 2000). Since total COD was represented by glucose, according to (John et al. 2020), the proportion of each fraction was defined to be: SF 94.4%, SI 2.8%, XI 2.8%, XS and SA is 0%. All components in influent set to the boundary are aqueous (mobile).

The initial concentrations of all simulated components and bacterial groups in wetland were set to values zero to recreate the start-up situation and to reduce the impact of imposed initial conditions on bacteria distribution. The initial condition was eliminated in about 30 days.

The treatment performance in different seasons, the time series of water temperature, shown in Fig. 4, were brought into simulations as the forcing term.

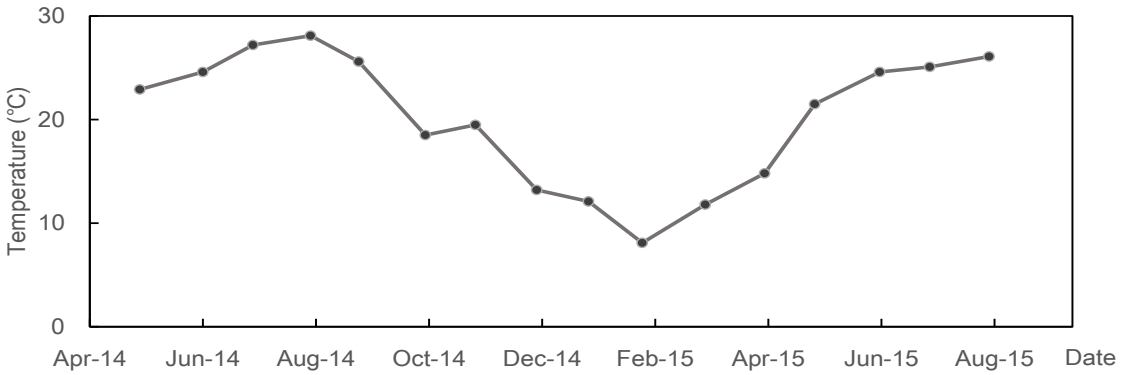


Fig. 4 Time series of water temperature during the simulated period

The material properties of 3 kinds of substrates filler (Fig. 1) in each layer are described by van Genuchten model, and the saturated permeability was calculated by the empirical formula utilized the grain size and porosity (Odong 2007). The parameter or coefficient values are listed in Table 1. The dispersion of mass transport at longitudinal and

transverse direction are 0.4 m^2s^{-1} and 0.01m^2s^{-1} respectively. There is no trace experimental data is available for calibration.

Table 1. Parameter values of material properties in 3 substrate layers

Layer	Thickness (cm)	Particle size (mm)	n	k (m^2)	α	m	θ_r	θ_s
1st	35	2-4	0.4	1.97×10^{-6}	14.5	4	0.01	1.0
2nd	25	2-4	0.45	2.90×10^{-6}	14.5	4	0.01	1.0
3rd	30	4-8	0.45	1.16×10^{-6}	14.5	4	0.01	1.0

The two main aspects of plant effects in modelling are considered as ROL and IOC, which are switched off in the no-plant (NP) modelling, and switched on in with plants (WP) case. The CWM1 model possesses amount of parameters, and most parameter values in the paper are from published references (Langergraber et al. 2009, Toscano et al. 2009) (Samsó and Garcia 2013b), some are calibrated by experimental data. Besides the inherent ones, the parameter values of ROL and internal organic carbon (IOC) loading from plant roots are from references and calibration. The aeration by intermittent influent is calibrated by the data of unplanted IVCW experiment. The important parameters are listed in Table 3.

Table 2. Parameters calibrated or referenced in the model.

Parameters	Description	Value	Source
Aeration (OTR+ROL)			
$k_{La,A}$	Coefficient in OTR of unsaturated zone, h^{-1}	7	-
$k_{La,R,down}$	Coefficient in OTR in down-flow chamber, h^{-1}	0.8	-

$k_{La,R,up}$	Coefficient in OTR in up-flow chamber, h^{-1}	0.37	-
D_{lo}	Diffusion coefficient for S_O for ROL, $m^2 s^{-1}$	2.4×10^{-9}	9.9×10^{-10}~2.66×10^{-9} (Cook and Knight 2003)
L_0	Root length density at z=0m, $m^3 m^{-3}$	10^5	10^2 ~10^5 (Cook and Knight 2003)
α_o	Bunsen adsorption coefficient, -	0.8	0.291~ 0.489 (Cook and Knight 2003)
S^*_{root}	S_O at the root surface, mg O_2 L^{-1}	2	1~10 (Cook, 20103)
Z_r	Scaling depth, m	0.12	0.1~1.0 (Cook and Knight 2003)
Internal organic loading from root exudate			
K_{root}	Carbon release from plants roots, mg L^{-1} d^{-1}	7.2	Calibration
θ_{carbon}	Coefficient of correcting K_{root} by temperature, -	1.1	Calibration
Ammonia absorption			
S_{Max}	Maximum amount of adsorbed concentration, kg kg^{-1}	0.00135	(Lu et al. 2016)
K_L	Coefficient of Langmuir, m^3 kg^{-1}	0.0145	(Lu et al. 2016)
Calibrated parameters in CWM1			
$M_{max,bio}$	Microbial reproduction over the medium impedes bacterial growth, g COD L^{-1}	2.7	Calibration
M_{cap}	Restriction of bacterial growth by particulate matter attached to the medium, g COD L^{-1}	40	Calibration

η_g	Correction factor for denitrification by heterotrophs, -	1	0.8 (Langergraber et al. 2009, Toscano et al. 2009)
K_{OH}	Saturation/inhibition coefficient for S_O, mg O_2 L^{-1}	2	0.2 (Langergraber et al. 2009)
K_{NHA}	Saturation/inhibition coefficient for S_{NH}, mg N L^{-1}	1.5 (20℃)/ 4.0 (10℃)	0.5 (20℃)/ 5.0 (20℃) (Langergraber et al. 2009)

In the experiment, the concentration of effluent and the water inside the wetland was sampled and measured. The comparisons of measured effluent concentrations of COD, NH_4-N and TN with simulated concentrations without and with plant (abbreviation for 'NP' and 'WP') during May 2014 to Aug 2015 are shown in Fig. 5. The measured variables are denoted by the symbols and the computed results are indicated by lines.

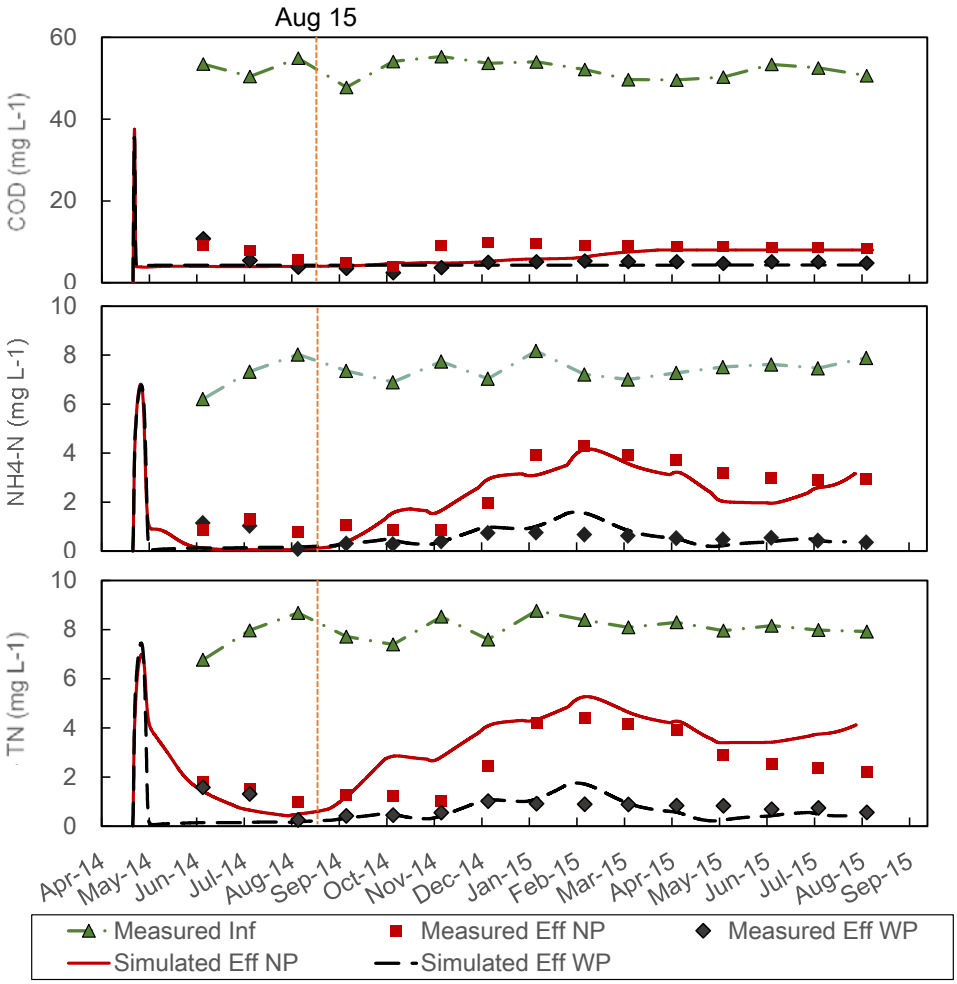


Fig. 5. Experimental influent and effluent concentrations (diamonds, deltas and squares) and the simulated effluent concentrations with plant and without plant effects (red solid and black dash line) during modelling period. (a) COD (mgO_2 L^{-1}), (b) NH_4–N (mg N L^{-1}) and (c) TN (mg N L^{-1}).

The inflow COD, NH_4-N and TN are reduced by both laboratory-scale IVCWs, and the planted IVCW has better treatment performance than unplanted one in the whole year, that is indicated by the measurements and the simulated results. The COD removals are considerably high (>85%) in both with and without plant IVCWs during the operating period. The nitrogen removals are highest in summer and lowest in winter. The lowest removal appears in Feb 2015. The contrasts of NH_4-N and TN removal between IVCWs with and without plant are remarkable in winter, which planted IVCW has 75-85% removal

rates and unplanted IVCW has 40~50% rate. It is consistent with many practical applications and experiments that the nitrogen removal variation along with the seasons in treating nitrate-laden wastewater of CWs (Boog et al. 2019). The season's efficiency of nitrogen removal from high to low are in the turn of summer, autumn spring and winter (Chang et al. 2013). The treat performance of nitrogen decreases in second year, shown by both measurements and simulations, which may due to the small size of IVCW, and the fast development of clogging process.

In terms of the effluent concentrations in the first year summer, there is no significant difference between the planted and unplanted IVCW. The interior water was sampled and measured in August 2014 for inside investigation (in Fig. 1). The simulated COD, NH_4-N, TN and DO along the polyline in Fig. 3 are plotted and compared with the measured data in Fig. 6. The polyline passes through the down-flow chamber (DFC), the bottom (BOT) and the up-flow chamber (UFC), which are denoted in Fig. 6.

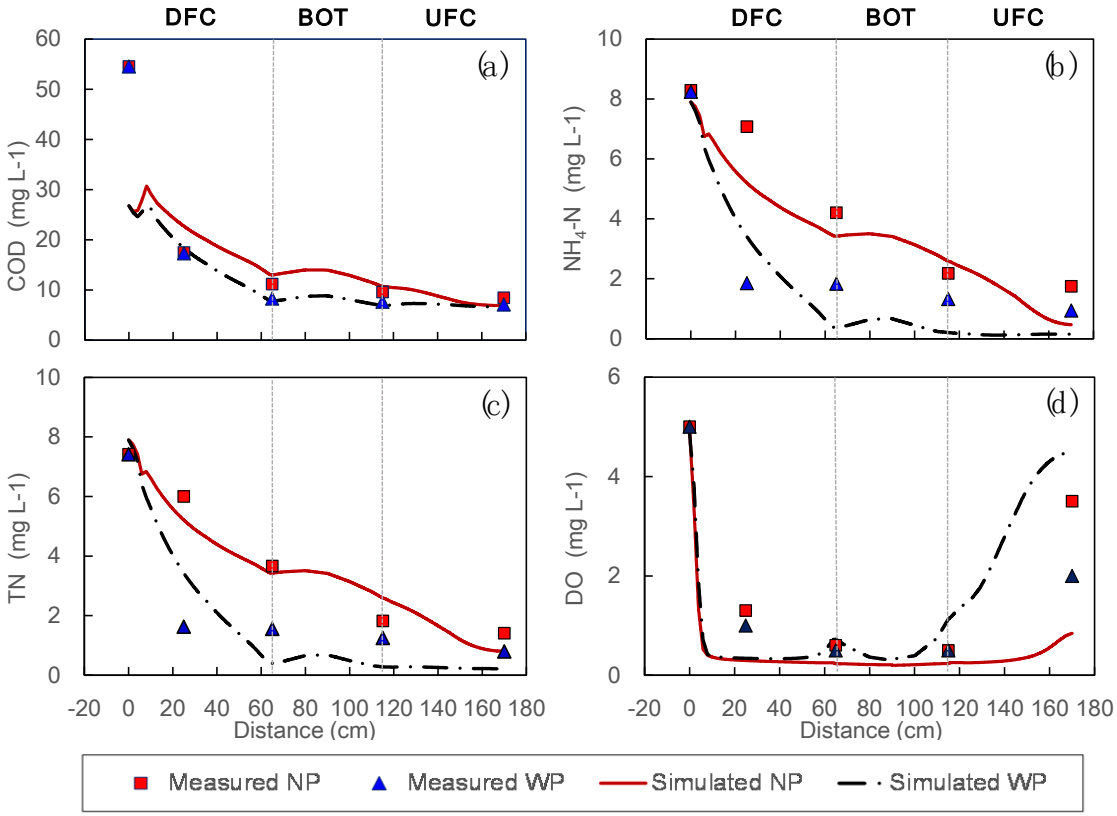


Fig. 6. Experimental data of without and without plants (deltas and squares) comparing with simulated results along polyline without plant effects (red solid line) and with plant effects (blue dash line) on Aug 15th 2014 for (a) COD ($mgO_2\ L^{-1}$), (b) NH_4–N (mg N L^{-1}), (c) TN (mg N L^{-1}) and (d) DO (mg $O_2\ L^{-1}$).

High levels (96 and 97%) of COD were successfully removed from artificial wastewater by two laboratory-scale IVCWs with plants and without plant, respectively. Although subtle differences between the effluent of NP and WP IVCW appear in Fig. 6 in August 2014, the interior differences of nitrogen are remarkable. The COD, NH_4-N and TN decreases gradually along the flow stream in both IVCWs. The COD profile in planted IVCW is similar with that in unplanted one. The concentrations of NH_4-N and TN in down-flow chamber and bottom in NP IVCW are higher than those in WP CW. In planted IVCW, the NH_4-N and TN are removed about 80% in down-flow chamber, and the reduction of the rest nitrogen become slowly. As the contrary, the removals of nitrogen in down-flow chamber in NP IVCW are about 50%, and the removal rates persist in bottom and up-flow chamber. NH_4-N and TN in the down-flow chamber decreases more rapidly in WP than in NP CW.

The laboratory-scale IVCWs fed by intermittent wastewater exhibit the high efficiency of COD and nitrogen removal. There are sufficient DO for the degradation of COD and NH_4-N in both IVCWs. Additionally, the effluent DO indicates the differences between NP and WP IVCWs in Fig. 6. Down-flow chamber in IVCW is the area for DO consumption resulting the similar DO profiles from the surface to bottom in both CWs. DO rises in UFC from the bottom to surface, and DO in WP is higher than that in NP at the outlet.

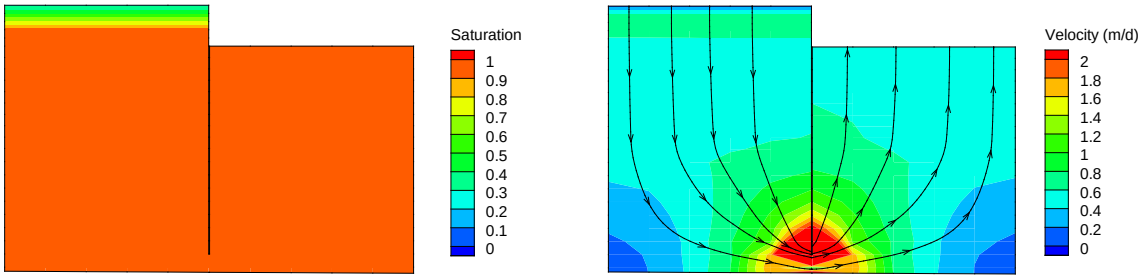
In general, the simulated time serial of effluent and profiles of COD, NH_4-N and TN in summer in both IVCWs are in agreement with the measured data, which proves the reasonable setting for plant effects in model.

460 *3.2 Discussion*

461 3.2.1 Hydrodynamics and water quality in IVCW

462 The measurements are applied for the model calibration and validation, while
463 modelling results provide the spatiotemporal data of variables to investigate the relationship
464 between those variables. There is no distinct hydrodynamic difference in the planted and
465 unplanted CWs due to the model settings, and the simulated distributions of saturation and
466 flow speeds in IVCWs are shown in Fig. 7 (a) and (b).

467



(a) (b)

Fig. 7 Distribution of saturation (a), flow field (b) in IVCW

468

469 The substrates at surface layer in the down-flow chamber is unsaturated, the rest area is
470 saturated. In Fig. 7 (a), the domestic flow direction in two chambers are opposite. The highest
471 magnitude of flow speeds occurs at the joint area at bottom of two chambers, the lowest flow
472 speeds appears at ancipital bottom corners, where may form the dead zone in IVCW.

473 Under the steady hydrodynamic conditions, the bio-chemical processes form the spatial
474 distinct patterns of DO, COD, NH_4-N and TN in planted and unplanted IVCWs. The
475 distributions of DO, COD, NH_4-N and TN in Aug 15th 2014 in the unplanted IVCW are
476 selected and shown in Fig. 8.

477

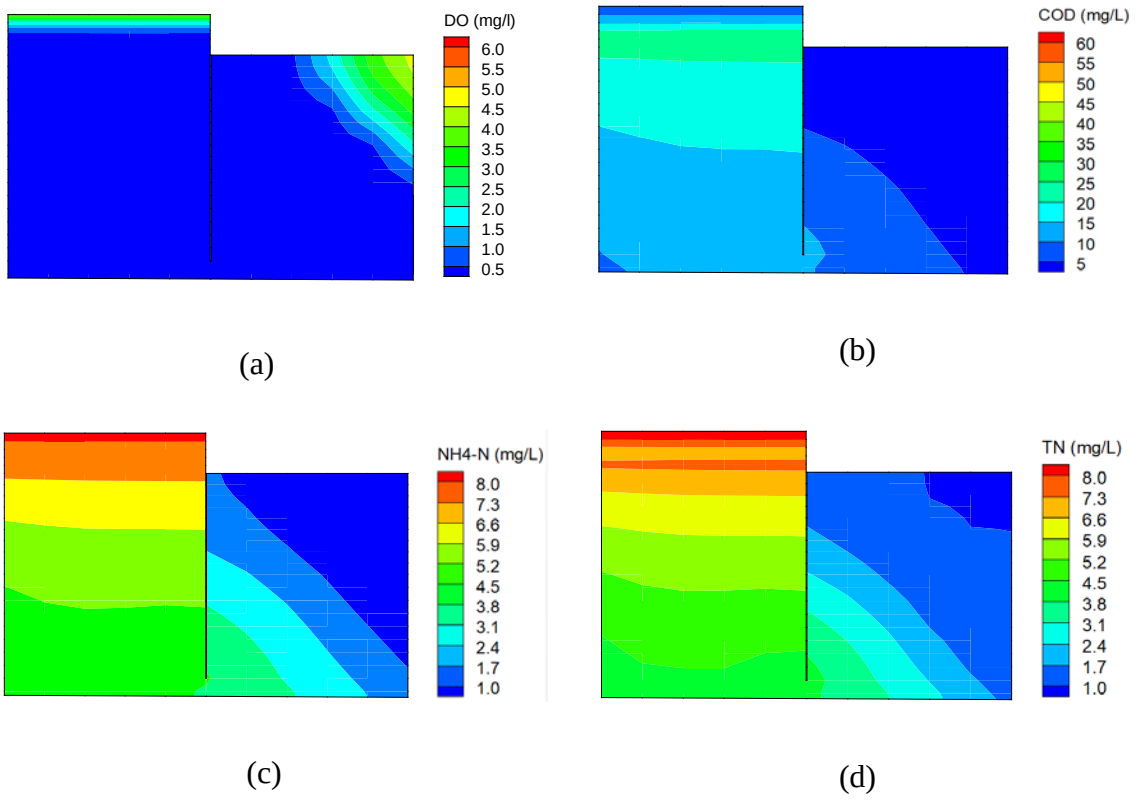


Fig. 8. Distributions of DO(a), COD(b), NH_4-N (c) and TN (d) on Aug 15th 2014 in unplanted IVCW

478

479 The intermittent influent generate the partially unsaturated zone in the top layer of CWs
480 that possess high oxygen transfer capacity, and boosts the nitrification reaction. The
481 concentration of COD, NH_4-N and TN decrease following the flow streams from down-flow
482 chamber to up-flow chamber, in which COD drops faster than NH_4-N and TN. The aerobic
483 and anoxic conditions alternately exist in IVCWs as seen in Fig. 8.

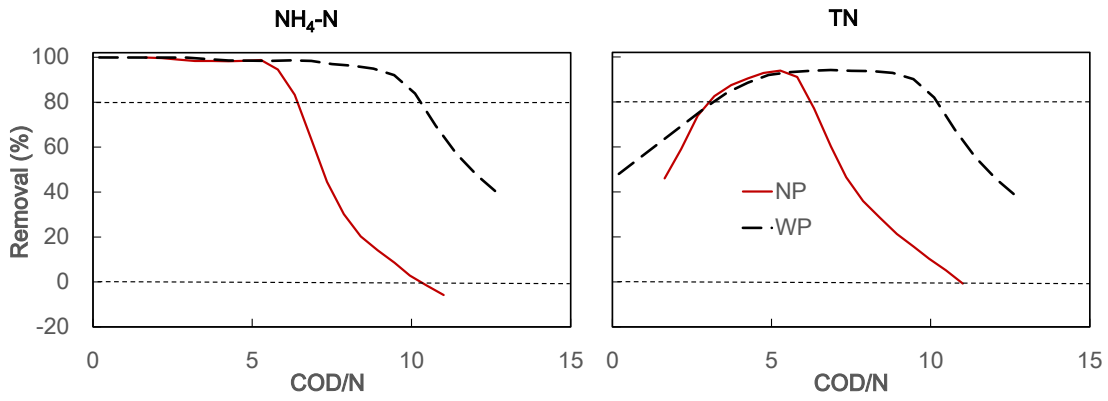
484 In practice applications, both horizontal subsurface flow (HSSF) CWs and IVCWs
485 have been widely employed to treat polluted surface water or domestic waste water (Chang et
486 al. 2013). Due to the structural differences, IVCWs provide the meandering flow and
487 aerobic-anoxic-aerobic alternately conditions for nitrification and denitrification, while
488 HSSF CWs offers the smooth horizontal flow and predominant anoxic condition for

489 denitrification. Therefore, which kind of CWs should be designed and applied for the
490 treatment partly is based on the nitrogen component of the influent.

491 3.2.2 Nitrogen removal with COD/N ratios in unplanted and planted IVCWs

492 The proper quantities of organic carbon feeding into the CWs can overcome the
493 limitations of deficient carbon loading to support denitrification and upgrade the nitrogen
494 removal performance (Ingersoll and Baker 1998, Chang et al. 2013). The COD/N ratio at
495 2.5 showed highest TN removal in Zhao et al. (2010), while in the other researches, the
496 proper COD/N ratios in a range of 2.5–20 in Fan (2013), and 6 in (Ding et al. 2012). The
497 influent COD/N ratio are related to DO supply which may affects the balance between
498 nitrification and denitrification in CWs, and COD/N ratios in a range of 2-20 (Wang et al.
499 2020) , and COD/N ratios at 10 in Wu et al. (2016). The COD/N ratios to promote nitrogen
500 removal alter with plantation, temperature, wetland configurations, aeration, nitrogen
501 composition, therefore it is not universal value(Saeed and Sun 2012).

502 N removal show different in unplanted and planted IVCWs in section 3.2.1. To explore
503 the appropriate influent COD/N for nitrogen removal, a series of COD/N ratios for
504 unplanted and planted CWs respectively are simulated. The constant temperature at 25℃
505 and same parameters setting in section 3.1 are employed in the models. The first scenario
506 presents the unplanted CW, and the second scenario presents the planted CW. Both
507 simulations run two months period for analysis. The removal of NH_4-N and TN along
508 COD/N ratios under unplanted and planted IVCWs are plotted in Fig. 9.



509

510 **Fig. 9.** Simulated NH_4-N (left) and TN (right) removal against COD/N ratio of unplanted

511 and planted IVCWs

512

513 In the intermittent feeding waste water, NH_4-N is predominant component in the

514 nitrogen composition. The 80% removal is set as the high treating performance. The high

515 NH_4-N removal are at COD/N < 7.2 in NPCW and COD/N < 10.5 in WPCW, which are the

516 threshold values for NH_4-N removal. If COD/N is larger than the threshold values, the

517 removal drops fast. When COD/N ranges in 4-7 in NPCW and in 3-10 in WPCW, TN are

518 treated efficiently, and the ratio range of WPCW are wider than that of NPCW. The lower

519 COD/N ratios indicates deficient carbon for bacteria growth and restricts denitrification,

520 while higher COD/N ratios causes high DO consuming, consequently inhibits the

521 nitrification, and both situations results low TN removal.

522 The COD/N ratio of influent in the experiment is about 6.0-7.1, which approaches the

523 upper limitation of the high nitrogen removal of unplanted CW. The organic loading is

524 sufficient for the nitrification in NPCW, however it is in the appropriate range of WPCW.

525 The IVCW with plants can tolerate the large changes of carbon loading and maintain the

526 high treat performance, which have been observed by experiments (Huett et al. 2005, Zhu et

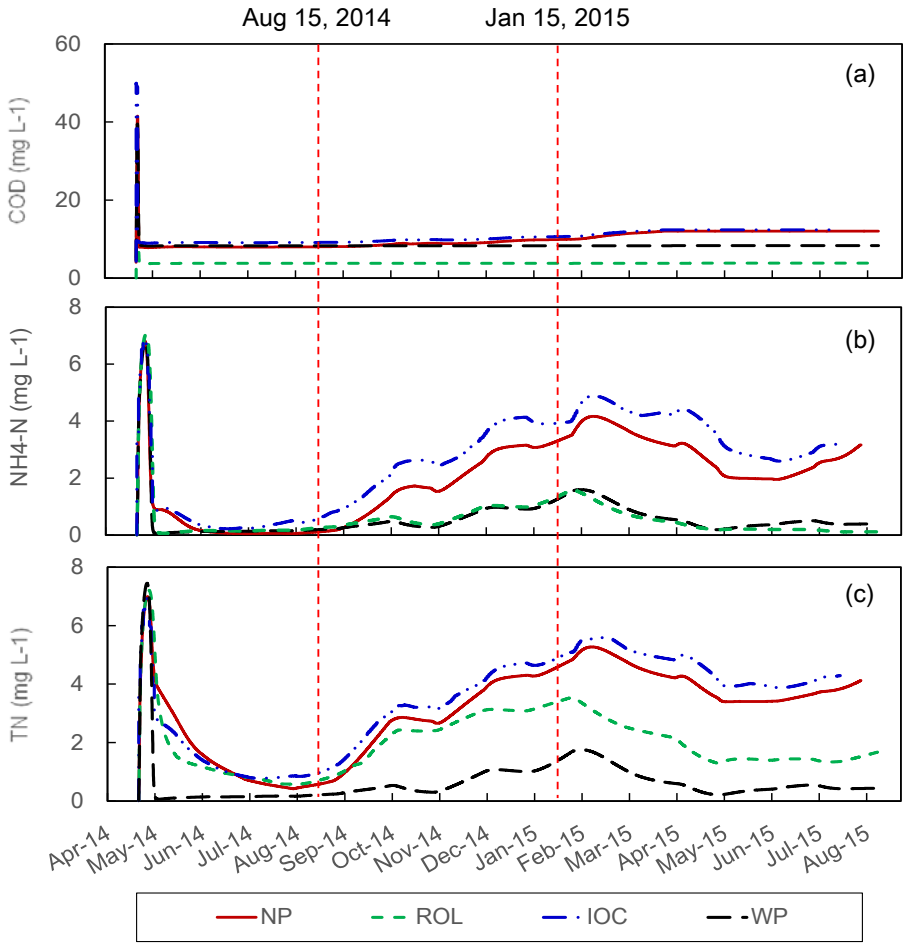
527 al. 2014).

528 3.2.3 Effects of plants and temperature on treatment performance

529 The combined two aspects of plants root as ROL and IOC introduced in section 2.2.3
530 are set in the model for WP computations in section 3.2.1. DO is a crucial factor for
531 treatment, and ROL function was already mentioned and simulated by (Langergraber and
532 Šimůnek 2012, Saeed and Sun 2013, Samsó and Garcia 2013a) . The increasing DO from
533 ROL enhances the removal of COD and NH4-N in CW system, while in low temperature
534 condition, increasing DO may weaken the TN the removal (Boog et al. 2019).

535 In order to investigate the contributions of ROL and IOC separately in treatment, based
536 on the NP model, ROL only and IOC only are added and employed in modelling. The
537 comparisons is consists of 4 cases abbreviated as “NP”, “ROL”, “IOC” and “WP”, and the
538 WP case combines the function of ROL and IOC as before. The boundary conditions and
539 the parameters setting in the model are identical with those in section 3.1.

540 The time series of effluent results of 4 cases are exhibited in Fig. 10, by red solid line,
541 green dash line, blue dash dot line and black long dash line, respectively.



542

543 **Fig. 10.** Simulated time series of effluent concentrations of NP, ROL, IOC and WP

544 cases during modelling period. (a) COD (mgO_2 L^{-1}), (b) NH_4–N (mg N L^{-1}) and (c) TN

545 (mg N L^{-1}).

546

547 The removal varied in the year corresponds to seasons. The activity of bacteria is

548 weakened at low temperature, therefore DO consumption decreased, especially by

549 nitrifying bacteria. The sufficient DO levels inhibited the activity of denitrifying bacteria

550 X_H and decreased NO_X-N removal.

551 Compared to the NP case, the ROL function promote the removal of COD, NH_4-N

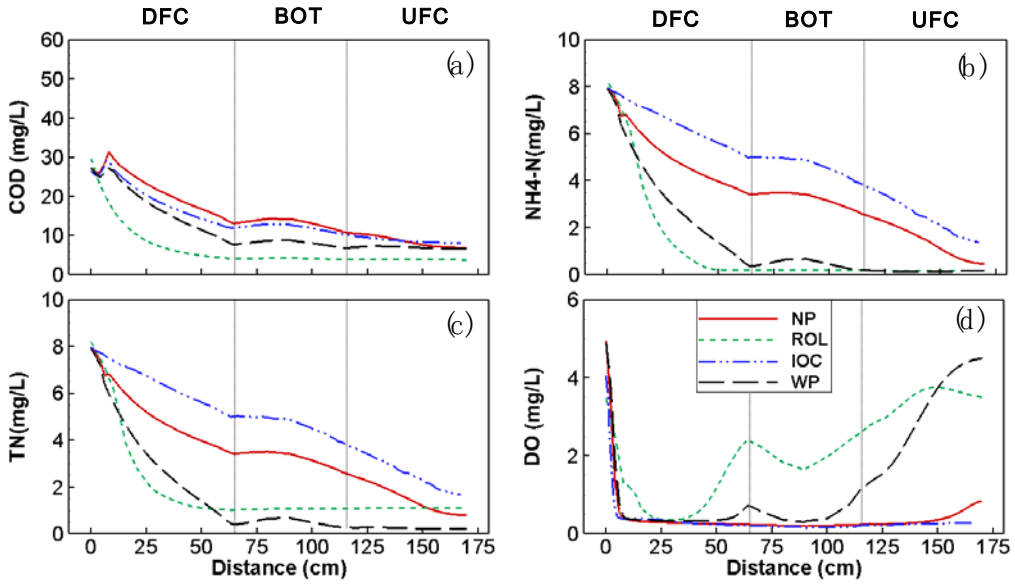
552 significantly especially in winter, which is similar to WP case. As for the TN removal, the

553 promotion by ROL are unremarkable against WP. In the sometime of summer, TN removal

554 by ROL is slightly higher than NP based on the comparative high removal. ROL vitalizes

555 the heterotrophic bacteria X_H and autotrophic nitrifying bacteria X_A to reduces the COD and
556 nitrify NH_4-N, nevertheless, it might inhibit the denitrification process and decrease the
557 NO_X-N removal. The computed the COD and NH_4-N concentration of effluent in ROL
558 cases are approximate to the WP case, while the TN values in winter and next year are high
559 than that in WP. The function of IOC drags down the removals. IOC in the substrates
560 consumes oxygen and depress the elimination of COD, NH_4–N and TN. The compound
561 function of ROL and IOC achieves the best performance. The order of removal efficiency
562 from low to high is IOC, NP, ROL and WP.

563 Two typical moments for summer and winter are selected to study the temperature
564 impacts (in Fig. 10). The concentration of COD, NH_4-N, TN and DO along the polyline
565 inside the IVCW on August 15th 2014 for 4 simulation cases are exhibited in Fig. 11.



566

567 **Fig. 11.** Simulated results along polyline of NP, ROL, IOC and WP cases on Aug 15th
568 2014. (a) COD (mgO_2 L^{-1}), (b) NH_4–N (mg N L^{-1}), (c) TN (mg N L^{-1}) and (d) DO (mg O_2
569 L^{-1}).

570

571 All IVCWs operate well in summer with the low contaminate concentration in effluent.
572 The profiles of COD, NH_4-N, TN and DO in NP and IOC case are approximate, although

the concentrate value are little higher in IOC case than those in NP case. IOC lowers DO demand for nitrification and COD removal along flow way, since IOC is evenly distributed in IVCW. The ROL and WP cases, most COD, NH4-N and TN from influent are eliminated powerfully in the DFC with the dropping DO, consequently DO escalates due to the less residual pollutants to be treated in the UFC.

Taking the NP case as a reference, DO changes (ΔDO) in ROL, IOC and WP cases in the whole domain are displayed in Fig. 12.

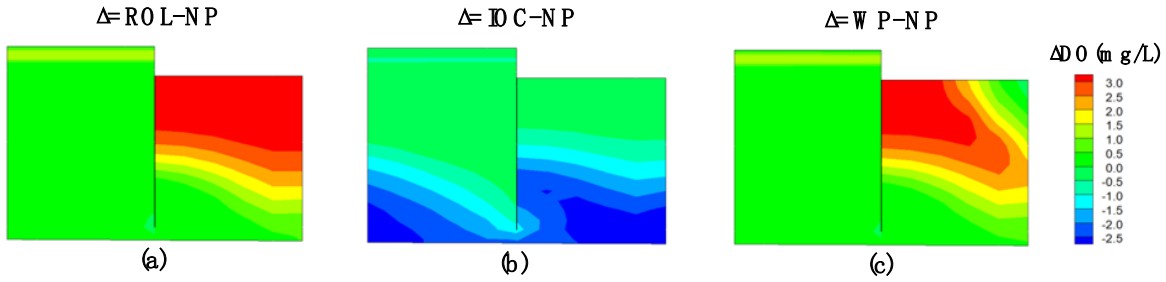
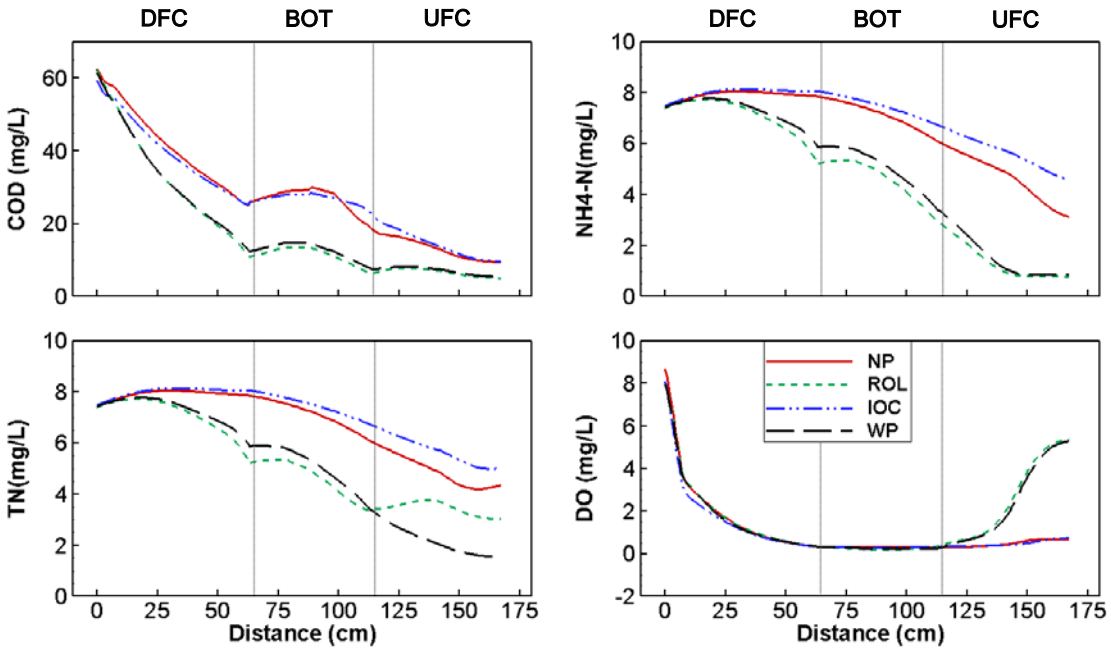


Fig. 12. DO changes (ΔDO) distribution of ROL, IOC and WP against with NP in IVCWs. (a) Δ=ROL-NP (mgO_2 L^{-1}), (b) Δ=IOC-NP (mgO_2 L^{-1}), and (c) Δ=WP-NP (mg O_2 L^{-1}).

Under the function of ROL, DO increases slightly in the top thin layer of down-flow chamber, and rises obviously in the half upper layer of up-flow chamber, indicated in Fig. 9(a). Without the ROL supply, OTR provides DO for biochemical reaction and transport through the flow in Fig 6. IOC in substrates causes the competition of DO consumption and aggravates the DO deficiency at bottom in IVCW (in Fig 9(b)). The combination function of ROL and IOC, DO ascends in some area in the upper layers.

In winter, the treat performance declines with the descent temperature. The concentration of COD, NH4-N, TN and DO along the polyline inside the IVCW on Jan 15th 2015 for 4 simulation cases are exhibited in Fig. 13.

595



596

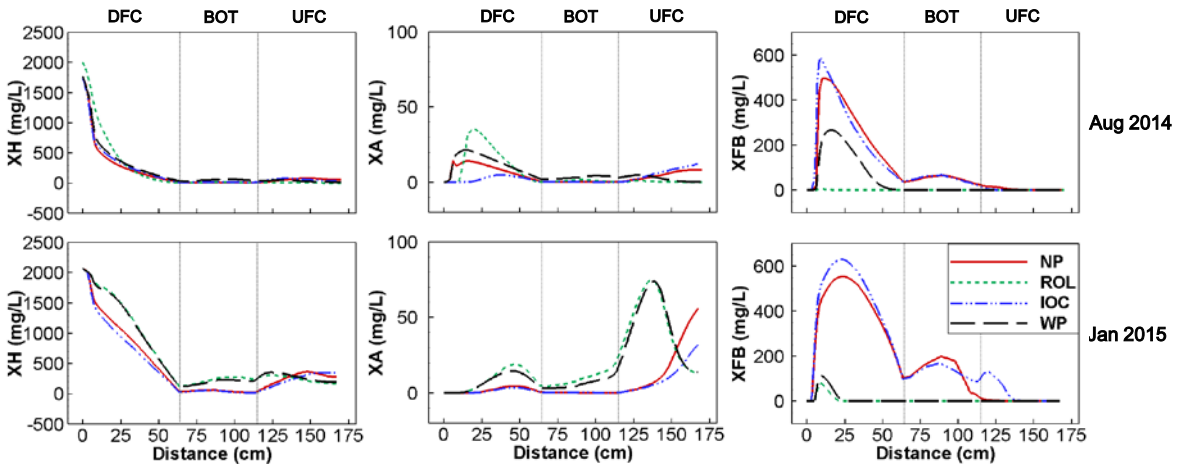
597 **Fig. 13.** Simulated results along polyline of NP, ROL, IOC and WP cases on Jan 15th
598 2015. (a) COD (mgO_2 L^{-1}), (b) NH_4–N (mg N L^{-1}), (c) TN (mg N L^{-1}) and (d) DO (mg O_2
599 L^{-1}).

600

601 Comparing the performance in summer, COD removal declines slightly, while NH_4-N
602 and TN removal descend appreciably in winter. Going to the profiles, the IOC and NP
603 cases have similar pattern, and WP and ROL cases show the resemblance. In IOC and NP
604 cases about 61%~83% COD is ridded in DFC, and eventually the removal are about
605 85~92%. The NH4-N and TN increases about by 7% instead of decrease in DFC, then drop
606 slowly at bottom and UFC, decrease by 40%~60% at outlet. The NH4-N removal in WP
607 and ROL IVCWs keep high as 90%, and TN removal in ROL IVCW is 64% which is lower
608 than 81% in WP IVCW. The inhibition of nitrification is initiated with an increase in
609 carbon loads. (Wu et al. 2013)

610 In order to improve the understanding of the treat performance changes in seasons, the
611 distribution of heterotrophic bacteria (X_H), autotrophic nitrifying bacteria (X_A) and

612 fermenting bacteria (X_{FB}) along the polyline inside the IVCWs in summer and winter are
613 plotted in Fig. 12.
614



615

616 **Fig. 12**. Simulated bacteria of X_H, X_A and X_{FB} along polyline of NP, ROL, IOC and
617 WP cases on Aug 15th 2014 and Jan 15th 2015.
618

619 A large amounts of heterotrophic bacteria X_H accumulate at the surface of down-flow
620 chamber (DFC) in IVCW in Fig. 12. There is competition between the two X_H and X_A in
621 the substrate biofilm. In winter, the growth rate of X_H does not drop at low temperature,
622 while the growth of X_A was significantly inhibited (Gao et al. 2015). The competition
623 between X_H and X_A become intensified in low temperature condition. High density of X_H
624 lead to the high mortality and lysis, which generates a quantity of COD and NH_4-N
625 (Langergraber and Šimůnek 2005), in turns causes the slowing down removal of COD and
626 increasing NH_4-N in DFC. In winter, autotrophic nitrifying bacteria X_A reduces in
627 down-flow chamber on the contrast of high X_A in summer. Additionally the attachment of
628 particulate material also weaken the growth X_A in down-flow chamber. The spaces for X_A
629 growth is squeezed into up-flow chamber. In IOC cases, the oxygen is taken up not only by
630 the inflow COD but also the IOC forming the anoxia condition in down-flow chamber. DO
631 deficiency in down-flow chamber also transform the high fermenting bacteria X_{FB} in IOC

632 and unplanted CW. Part of COD is removed by X_{FB} through fermentation in anoxia
633 condition in down-flow chamber, which results higher X_{FB} concentration and slightly lower
634 X_H at some area in IOC cases comparing unplanted CW.

635 The increasing carbon loading enhances the consuming of limited DO and depress the
636 nitrifying bacteria X_A, additional, it strengthens the competition between X_H and X_A, while
637 X_H has greater advantages with higher growth rate against that of X_A. With the continuous
638 growing of COD/N, X_A were severely restricted and the nitrification capacity almost is
639 weakened and disappeared. A great amount X_H takes the advantage to reproduce and
640 consequently the lysis of high mortality brings NH_4-N, which is shown as the negative
641 removal.

642 In terms of main bacteria components in this model, produced by hydrolysis and high
643 oxygen transfer capacity, a large amount of X_H grows at the surface layer of the down-flow
644 chamber due to its high OLR in unsaturated zone. Below the 10 cm depth of down-flow
645 chamber, X_A begins to grow and consume the oxygen, which accord with the decreasing
646 oxygen in the down-flow chamber. The concentration of total bacterial is highest at the
647 surface layer of the down-flow chamber due to the high pollution loads, and the mass of
648 bacteria in down-flow chamber takes the majority share of the system.

649 The influent organic feeding is sufficient or slightly excessive for nitrogen removal in
650 unplanted CW, though the COD/N ratio analysis in section 3.2.2. The additional internal
651 organic carbon (IOC) in unplanted CW without ROL decreases the NH_4-N and TN removal,
652 while the integration function of IOC and ROL in planted CW upgrades the performance,
653 which are coherent to the results in section 3.2.3.

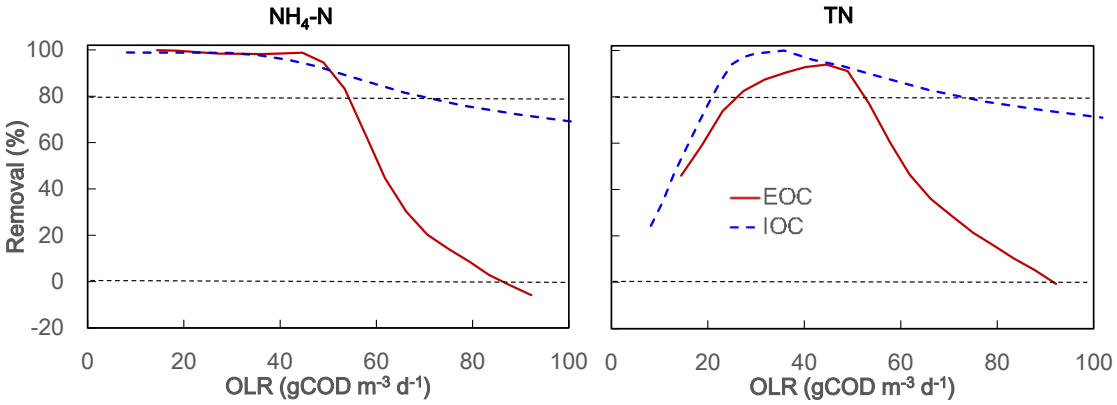
654 3.2.4 Influence of internal organic carbon on treatment performance

655 The deficient carbon loading cause the low nitrogen removal is the common problem of
656 CW operation in China. In addition to the adjustment of influent COD/N, the filler

657 selections for increasing carbon sources are widely studied (Saeed and Sun 2012, Saeed and
658 Sun 2017, Wang et al. 2017, Xu et al. 2019). The IOC including the exudation from plant
659 roots, filler releases, can significantly fuel the nitrogen removal. The impacts of the
660 quantification IOC on treatment are difficult to evaluate accurately by experiment while it
661 can be calculated by model.

662 The IOC released from filler (including plant roots) show the spatial distinction from
663 the external organic carbon (EOC) from influent, which may generate the different treating
664 performance. In order to investigate the IOC and EOC effects on treatment performance.
665 Assuming the constant temperature at 25℃, OTR level as same as the section 3.1, and
666 ignoring the ROL, the hypothetical organic carbon loading rates (OLR) was simulated at
667 different levels in two scenarios. The first scenario (I) consisted in a set of simulations with
668 same initial condition, nitrogen loading, oxygen transfer rate, temperature and zero IOC
669 loading during the cross-validation scenario except the influent COD loading as EOC is set
670 to different constant values in each simulation. In the second scenario (II), EOC is switched
671 to zero and IOC is set to varied values, while the rest settings are identical to scenario (I).
672 Each simulation lasts 60 days to reach the steady-state status for analysis.

673 The nitrogen in the system removal changes with the increasing external or internal
674 organic loading rates (OLR), shown in Fig. 13. The red solid lines indicates the removal of
675 NH_4 and TN under EOC inflow conditions, and blue dash lines denotes the IOC conditions.



676

677

678 **Fig.13.** Simulated removal of NH_4-N and TN against loading rates of EOC and IOC.

679

680 In scenario (I) when the OLR is lower than 40 gCOD $m^{-3}d^{-1}$, NH_4-N removal achieves
681 above 95%, and when OLR is greater than 40 gCOD $m^{-3}d^{-1}$, removal drops sharply with
682 the10 gCOD $m^{-3}d^{-1}$ OLR amplification decreasing 35~47% removal. When OLR is over 80
683 gCOD $m^{-3}d^{-1}$, the removal become negative, which means the effluent NH_4-N is larger than
684 the influent. Similarly, low OLRs in scenario (II) lead to the high NH_4-N removal, the point
685 of inflection is at 30 gCOD$m^{-3}d^{-1}$. Nevertheless, the removal decline rates is significantly
686 greater in scenario (I) than those in scenario (II).

687 Higher organic loading enhances the consuming of limited DO and depress the
688 nitrifying bacteria X_A, additional, the increasing carbon loading strengthen the competition
689 between X_H and X_A, while X_H has greater advantages with higher growth rate of X_H against
690 that of X_A. With the continuous growing of OLR, X_A were severely restricted and the
691 nitrification capacity almost is weakened and disappeared. A great amount X_H takes the
692 advantage to reproduce and consequently the lysis of high mortality brings NH_4-N, which is
693 shown as the negative removal. Under the higher OLR status (larger than 45 gCOD $m^{-3}d^{-1}$),
694 the IOC loading in IVCWs shows higher efficiency to remove NH_4-N than EOC loading.

695 Simulated TN removal appears a single-peak pattern with the increasing OLR in both
696 scenarios. The peak value of TN removal is about 93% with the EOC loading at 42
697 gCOD$m^{-3}d^{-1}$ in scenario (I), and the peak removal reaches 99% with the IOC loading at 30
698 gCOD $m^{-3}d^{-1}$ in scenario (II). Under the same OLR condition, the TN removal in scenario
699 (I) is higher than that in scenario (II). Wherever the organic carbon from, lower EOC or
700 IOC results the decrease of denitrifying bacteria X_H due to carbon deficiency, which
701 deteriorates denitrification of NOx-N and increases effluent NOx-N concentrations. Under
702 higher OLR condition, comparing with EOC cases, the uniform distribution of IOC relieve
703 the DO consuming at the inlet area, which helps the nitrification of NH_4-N in down-flow

chamber and denitrification of NOx-N at bottom and in up-flow chamber. Therefore the TN removal is higher in scenario (I) than that in scenario (II).

Low OLR influent brings out the low TN removal in IVCWs, and the additive organic carbon in substrate in the bottom and up-flow chamber can improve the treat performance powerfully. The filling material section and assembling in CW can be well designed by the numerical model for the best performance.

4. Conclusions

The integrated vertical constructed wetlands (IVCW) normally have a strong aeration capability and powerful remediation performance, are widely applied for the waste water treatment. Based on the main functions of the wetland plants, the radial oxygen loss (ROL) and internal organic carbon (IOC) exudates from roots are mathematically described and implemented in the CWM1 model to simulate plant effects on the remediation performance. A novel model combination (OpenGeoSys#IPHREEQC) has been implemented and used for the analysis of experimental results. This model combination allows the analysis and interplay of aeration, internal organic carbon (IOC) loading from root exudate, ammonia absorption, clogging and limitation of biomass processes for the elucidating the remediating efficiency of IVCW under a broad range of conditions. The model is calibrated and successfully validated by measured experimental data, presenting the removal improvement by the plants. The removal of NH_4-N and TN decrease remarkably in low temperature condition especially for unplanted IVCW, while the function of plants roots counteract the effect of low temperature partly in planted IVCW.

Although there is no universal COD/N ratio for all CWs, the optimal COD/N ratios for high TN removal of planted and unplanted IVCWs are obtained by the model simulation instead of numerous experiments. The COD/N ratio can be used to evaluate the carbon loading levels for nitrogen removal. When the carbon loading reaches an the upper limit,

single factor of ROL can support the COD, NH_4-N removal, and preserve the TN removal at elevated temperatures, while it may inhibit the denitrification and decrease TN removal at lower temperatures. The additional IOC enhances the oxygen consuming and lower the COD, NH_4-N and TN removal. The combination of ROL and IOC can improve the treat performance.

Generalizing all the organic carbon released by roots or substrates as IOC, the quantified IOC impacts on the treat performance are calculated and compared with the EOC effects. The IOC yields higher TN removal performance than the EOC at the same loading, because of the different spatial characteristics. The coupled model systems provides a useful tool for a better understanding the complex interplay of biogeochemical and hydraulic processes under variable saturation and, therefore, allowing for better design and optimal operation of CWs.

Funding:

This work was jointly supported by the Major Science and Technology Program for Water Pollution Control and Treatment (No.2017ZX07101004) and Research & Development Support Program of

Acknowledgments:

This work was funded by the Major Science and Technology Program for Water Pollution Control and Treatment (No.2017ZX07101004) and NFSC project (Ref. 51861135314). The authors gratefully acknowledge the OGS team leading by Prof Kolditz.

Conflicts of Interest:

References

1. Akizuki, S., Wong, T.K., Aoki, Y., Cuevas-Rodríguez, G., Niwa, C. and Toda, T. (2015) Effects of substrate COD/NO2−-N ratio on simultaneous methanogenesis and short-cut denitrification in the treatment of blue mussel using acclimated sludge. Biochemical Engineering Journal 99, 8.
2. Bachand, P.A.M.a.H., A.J. (2000) Denitrification in constructed free-water surface wetlands: II. Effects of vegetation and temperature. Ecol. Eng., 14(1-2), 16.
3. Bilke, L., Flemisch, B. and Kalbacher, T.e.a. (2019) Development of Open-Source Porous Media Simulators: Principles and Experiences Transport in porous media 130(1), 25.
4. Boano, F., Rizzo, A., Samsó, R., García, J., Revelli, R. and Ridolfi, L. (2018) Changes in bacteria composition and efficiency of constructed wetlands under sustained overloads: A modeling experiment. Science of The Total Environment 612, 1480-1487.
5. Boog, J., Kalbacher, T., Nivala, J., Forquet, N., van Afferden, M. and Muller, R.A. (2019) Modeling the relationship of aeration, oxygen transfer and treatment performance in aerated horizontal flow treatment wetlands. Water Res. 157, 321-334.
6. Brix, H. (1997) Do macrophytes play a role in constructed treatment wetlands? Water Sci. Technol. 35 (5), 7.
7. Canarini, A., Kaiser, C., Merchant, A., Richter, A. and Wanek, W. (2019) Root Exudation of Primary Metabolites: Mechanisms and Their Roles in Plant Responses to Environmental Stimuli. Front Plant Sci 10, 157.
8. Carrasco-Acosta, M., Garcia-Jimenez, P., Herrera-Melián, J.A., Peñate-Castellano, N. and Rivero-Rosales, A. (2019) The Effects of Plants on Pollutant Removal, Clogging, and Bacterial Community Structure in Palm Mulch-Based Vertical Flow Constructed Wetlands. Sustainability 11(3).
9. Caspersen, S., Sundin, P., Aoalsteinsson, S., Jensen, P. (2004) A gnotobiotic system for studying root carbon release using lettuce (Lactuca sativa L.). Sci. Hortic.Amsterdam 99 (2)(14), 119.
10. Chang, J.-j., Wu, S.-q., Dai, Y.-r., Liang, W. and Wu, Z.-b. (2013) Nitrogen removal from nitrate-laden wastewater by integrated vertical-flow constructed wetland systems. Ecological Engineering 58, 192-201.
11. Charlton, S.R. and Parkhurst, D.L. (2011) Modules based on the geochemical model PHREEQC for use in scripting and programming languages. Computers & Geosciences 37(10), 1653-1663.
12. Chen, Z.-J., Tian, Y.-H., Zhang, Y., Song, B.-R., Li, H.-C. and Chen, Z.-H. (2016) Effects of root organic exudates on rhizosphere microbes and nutrient removal in the constructed wetlands. Ecological Engineering 92, 243-250.
13. Chen, Z.M., Chen, B., Zhou, J.B., Li, Z., Zhou, Y., Xi, X.R., Lin, C. and Chen, G.Q. (2008) A vertical subsurface-flow constructed wetland in Beijing. Communications in Nonlinear Science and Numerical Simulation 13(9), 1986-1997.
14. Clement, J.C., Pinay, G., Marmonier, P. (2002) Seasonal dynamics of denitrification along to pohydrosequences in three different riparian wetlands. J. Environ. Qual. 31 (3), 13.
15. Collison, R.S.a.M.E.G. (2014) Nitrogen and Chemical Oxygen Demand removal from septic tank wastewater in subsurface flow constructed wetlands: Substrate (Cation Exchange Capacity) effects. . Water Environment Research 86(4), 10.
16. Cook, F.J. and Knight, J.H. (2003) Oxygen Transport to Plant Roots: Modeling for Physical Understanding of Soil Aeration. Soil Sci. Soc. Am. J. 67, 12.
17. Cook, F.J., Knight, J.H. and Kelliher, F.M. (2013) Modelling oxygen transport in soil with plant root and microbial oxygen consumption: depth of oxygen penetration. Soil Research 51(6).
18. Ding, Y., Song, X., Wang, Y. and Yan, D. (2012) Effects of dissolved oxygen and influent COD/N ratios on nitrogen removal in horizontal subsurface flow constructed wetland. Ecological Engineering 46, 107-111.
19. Dundek, P., Holík, L., Rohlík, T., Hromádko, L., Vranová, V., Rejšek, K. and Formánek, P. (2011) Methods of plant root exudates analysis: a review. Acta Universitatis Agriculturae et Silviculturae Mendelianae Brunensis LIX(32), 6.

20. Fan, J., Wang, W., Zhang, B., Guo, Y., Nuo, H.H., Guo, W., Zhang, J. and Wu, H. (2013) Nitrogen removal in intermittently aerated vertical flow constructed wetlands: impact of influent COD/N ratios. Bioresour. Technol. 143, 6.
21. Gao, D., Huang, X., Tao, Y., Cong, Y. and Wang, X.-l. (2015) Sewage treatment by an UAFB–EGSB biosystem with energy recovery and autotrophic nitrogen removal under different temperatures. Bioresource Technology 181, 6.
22. GarcÍA, J., Rousseau, D.P.L., MoratÓ, J., Lesage, E.L.S., Matamoros, V. and Bayona, J.M. (2010) Contaminant Removal Processes in Subsurface-Flow Constructed Wetlands: A Review. Critical Reviews in Environmental Science and Technology 40(7), 561-661.
23. Giraldi, D., de Michieli Vitturi, M. and Iannelli, R. (2010) FITOVERT: A dynamic numerical model of subsurface vertical flow constructed wetlands. Environmental Modelling & Software 25(5), 633-640.
24. Greenway, M.a.W., A. (2001) Changes in plant biomass and nutrient removal over 3 years in a constructed wetland in Cairns, Australia. Wat. Sci. Tech. 44(11–12), 8.
25. Haichar, F.Z., Marol, C., Berge, O., Rangel-Castro, J.I., Prosser, J.I., Balesdent, J., Heulin, T. and Achouak, W. (2008) Plant host habitat and root exudates shape soil bacterial community structure. ISME J 2(12), 1221-1230.
26. Han, E., Merwade, V. and Heathman3, G.C. (2012) Application of Data Assimilation with the Root Zone Water Quality Model for Soil Moisture Profile Estimation in the Upper Cedar Creek, Indiana. Hydrologcial Process, 13.
27. Hang, L., Liang, Y.-k., Liang, Y., Luo, X. and Chen, Y.-c. (2019) Influences of Biochar Application on Root Aerenchyma and Radial Oxygen Loss of Acorus calamus in Relation to Subsurface Flow in a Constructed Wetland. Environmental Science（Chinese） 40(3), 7.
28. He, W., Beyer, C., Fleckenstein, J.H., Jang, E., Kolditz, O., Naumov, D. and Kalbacher, T. (2015) A parallelization scheme to simulate reactive transport in the subsurface environment with OGS#IPhreeqc 5.5.7-3.1.2. Geoscientific Model Development 8(10), 3333-3348.
29. Henze, M., Gujer, W., Mino, T., van Loosdrecht, M.C.M. (2000) Activated sludge models ASM1, ASM2, ASM2d and ASM3, Scientific and Technical Report No. 9, IWA Publishing Company, London, UK.
30. Hua, G., Cheng, Y., Kong, J., Li, M. and Zhao, Z. (2018) High-throughput sequencing analysis of bacterial community spatiotemporal distribution in response to clogging in vertical flow constructed wetlands. Bioresour Technol 248(Pt B), 104-112.
31. Huett, D.O., Morris, S.G., Smith, G. and Hunt, N. (2005) Nitrogen and phosphorus removal from plant nursery runoff in vegetated and unvegetated subsurface flow wetlands. Water Research 39(14), 3259-3272.
32. Ingersoll, T.L. and Baker, L.A. (1998) Nitrate removal in wetland mesocosms. Water Res. 32, 8.
33. John, Y., Langergraber, G., Adyel, T.M. and Emery David, V., Jr. (2020) Aeration intensity simulation in a saturated vertical up-flow constructed wetland. Sci Total Environ 708, 134793.
34. Kalbacher, T.S., C. L.; Wang, W.; et al. (2011) Modeling Soil-Coupled Water Uptake of Multiple Root Systems with Automatic Time Stepping Vadose Zone Journal 10(2), 9.
35. Kim, S.-Y.a.G., P.M. (2001) The impact of biomass harvesting on phosphorus uptake by wetland plants. Wat. Sci. Tech. 44(11-12), 7.
36. Kolditz, O., Bauer, S., Bilke, L., Böttcher, N., Delfs, J.O., Fischer, T., Görke, U.J., Kalbacher, T., Kosakowski, G., McDermott, C.I., Park, C.H., Radu, F., Rink, K., Shao, H., Shao, H.B., Sun, F., Sun, Y.Y., Singh, A.K., Taron, J., Walther, M., Wang, W., Watanabe, N., Wu, Y., Xie, M., Xu, W. and Zehner, B. (2012) OpenGeoSys: an open-source initiative for numerical simulation of thermo-hydro-mechanical/chemical (THM/C) processes in porous media. Environmental Earth Sciences 67(2), 589-599.
37. Kolditz, O., Goerke, U.J., Shao, H., Wang, W. and Bauer, S. (2015) Thermo-Hydro-Mechanical-Chemical Processes in Fractured Porous Media: Modelling and Benchmarking Springer International Publishing.
38. Kuzyakov, Y. (2002). Review: factors affecting rhizosphere priming effects. J. Plant Nutr. Soil Sci. 165 (4), 15.

39. Kyambadde, J., Kansiime, F., Gumaelius, L. and Dalhammar, G. (2004) A comparative study of Cyperus papyrus and Miscanthidium violaceum-based constructed wetlands for wastewater treatment in a tropical climate. Water Res. 38(11), 475.
40. Lai, W.-L., Zhang, Y. and Chen, Z.-H. (2012) Radial oxygen loss, photosynthesis, and nutrient removal of 35 wetland plants. Ecological Engineering 39, 24-30.
41. Langergraber, G., Rousseau, D.P., Garcia, J. and Mena, J. (2009) CWM1: a general model to describe biokinetic processes in subsurface flow constructed wetlands. Water Sci Technol 59(9), 1687-1697.
42. Langergraber, G. and Šimůnek, J. (2005) Modeling Variably Saturated Water Flow and Multicomponent Reactive Transport in Constructed Wetlands. Vadose Zone Journal 4(4), 924-938.
43. Langergraber, G. and Šimůnek, J. (2012) Reactive Transport Modeling of Subsurface Flow Constructed Wetlands Using the HYDRUS Wetland Module. Vadose Zone Journal 11(2).
44. Lima MX, C.K., Passig FH, Borges AC, Filippe TC, Azevedo JCR, Nagalli A (2018) Performance of different substrates in constructed wetlands planted with E. crassipes treating low-strength sewage under subtropical conditions. Sci Total Environ 630, 9.
45. Lin, Y.-F., Jing, S.-R., Wang, T.-W. and Lee, D.-Y. (2002) Effects of macrophytes and external carbon sources on nitrate removal from groundwater in constructed wetlands. Environ. Pollut. 119(3), 8.
46. Lu, R.W., Norihiro; He, Wenkui; et al. (2017) Calibration of water-granite interaction with pressure solution in a flow-through fracture under confining pressure Environmental Earth Sciences 76(12).
47. Lu, S., Wan, Z., Li, F. and Zhang, X. (2016) Ammonia Nitrogen Adsorption and Desorption Characteristics of Twenty-Nine Kinds of Constructed Wetland Substrates. Research of Environmental Sciences (Chinese) 29(8), 8.
48. Mburu, N., Sanchez-Ramos, D., Rousseau, D.P.L., van Bruggen, J.J.A., Thumbi, G., Stein, O.R., Hook, P.B. and Lens, P.N.L. (2012) Simulation of carbon, nitrogen and sulphur conversion in batch-operated experimental wetland mesocosms. Ecological Engineering 42, 304-315.
49. Mei, X.Q., Yang, Y., Tam, N.F., Wang, Y.W. and Li, L. (2014) Roles of root porosity, radial oxygen loss, Fe plaque formation on nutrient removal and tolerance of wetland plants to domestic wastewater. Water Res 50, 147-159.
50. Morvannou, A., Choubert, J.-M., Vanclooster, M. and Molle, P. (2014) Modeling nitrogen removal in a vertical flow constructed wetland treating directly domestic wastewater. Ecological Engineering 70, 379-386.
51. Nayar, S., Collings, G.J., Miller, D.J., Bryars, S. and Cheshire, A.C. (2010) Uptake and resource allocation of ammonium and nitrate in temperate seagrasses Posidonia and Amphibolis. Mar Pollut Bull 60(9), 1502-1511.
52. Nivala, J., Knowles, P., Dotro, G., Garcia, J. and Wallace, S. (2012) Clogging in subsurface-flow treatment wetlands: measurement, modeling and management. Water Res 46(6), 1625-1640.
53. Odong, J. (2007) Evaluation of empirical formulae for determination of hydraulic conductivity based on grain-size analysis. Journal of American Science 3(3), 7.
54. Pelissari, C., dos Santos, M.O., Rousso, B.Z., Bento, A.P., de Armas, R.D. and Sezerino, P.H. (2016) Organic load and hydraulic regime influence over the bacterial community responsible for the nitrogen cycling in bed media of vertical subsurface flow constructed wetland. Ecological Engineering 95, 180-188.
55. Philippot, L., Raaijmakers, J.M., Lemanceau, P. and Putten, W.H.v.d. (2013) Going back to the roots: the microbial ecology of the rhizosphere. NATURE REVIEWS：MICROBIOLOGY 11, 11.
56. Rajabzadeh, A.R., Legge, R.L. and Weber, K.P. (2015) Multiphysics modelling of flow dynamics, biofilm development and wastewater treatment in a subsurface vertical flow constructed wetland mesocosm. Ecological Engineering 74, 107-116.
57. Rousseau, L., Diederik, P., Vanrolleghem, P.A. and Pauw, N.D. (2004) Constructed wetlands in Flanders: a performance analysis. Ecological Engineering 23(3), 151-163.

58. Saeed, T. and Sun, G. (2012) A review on nitrogen and organics removal mechanisms in subsurface flow constructed wetlands: dependency on environmental parameters, operating conditions and supporting media. J Environ Manage 112, 429-448.
59. Saeed, T. and Sun, G. (2013) A lab-scale study of constructed wetlands with sugarcane bagasse and sand media for the treatment of textile wastewater. Bioresource Technology 128, 438-447.
60. Saeed, T. and Sun, G. (2017) Pollutant removals employing unsaturated and partially saturated vertical flow wetlands: A comparative study. Chemical Engineering Journal 325, 332-341.
61. Saeed, T., Sun, G. (2011a) A comparative study on the removal of nutrients and organic matter in wetland reactors employing organic media. Chemical Engineering Journal 171 (2), 9.
62. Saeed, T., Sun, G. (2011b) Kinetic modelling of nitrogen and organics removal in vertical and horizontal flow wetlands. Water Research 45, 16.
63. Samsó, R. and Garcia, J. (2013a) Bacteria distribution and dynamics in constructed wetlands based on modelling results. Sci Total Environ 461-462, 430-440.
64. Samsó, R. and Garcia, J. (2013b) BIO_PORE, a mathematical model to simulate biofilm growth and water quality improvement in porous media: Application and calibration for constructed wetlands. Ecological Engineering 54, 116-127.
65. Shi, J., Yang, Z., Dai, H., Lu, X., Peng, L., Tan, X., Shi, L. and Fahim, R. (2018) Preparation and application of modified zeolites as adsorbents in wastewater treatment. Water Sci Technol 2017(3), 621-635.
66. Stefanakis, A.I. and Tsihrintzis, V.A. (2012) Effects of loading, resting period, temperature, porous media, vegetation and aeration on performance of pilot-scale vertical flow constructed wetlands. Chemical Engineering Journal 181-182, 416-430.
67. Stottmeister, U., Wießner, A., Kuschk, P., Kappelmeyer, U., Kästner, M., Bederski, O., Müller, R.A. and Moormann, H. (2003) Effects of plants and microorganisms in constructed wetlands for wastewater treatment,. Biotechnol. Adv. 22 (1), 25.
68. Tanner, C.C. (2001) Plants as ecosystem engineers in subsurface-flow treatment wetlands. Wat. Res. Tech. 44, 10.
69. Tee, H.C., Lim, P.E., Seng, C.E., Nawi, M. (2012) Newly developed baffled subsurfaceflow constructed wetland for the enhancement of nitrogen removal. Bioresource Technology 104, 8.
70. Teixeira, D.L., Matos, A.T.d., Pimentel de Matos, M., Vieira, D.P., Araújo, E.D. and Ferraz, L.A. (2018) The influence of plant roots on the clogging process and the extractive capacity of nutrients/pollutants in horizontal subsurface flow constructed wetlands. Ecological Engineering 120, 54-60.
71. Toscano, A., Langergraber, G., Consoli, S. and Cirelli, G.L. (2009) Modelling pollutant removal in a pilot-scale two-stage subsurface flow constructed wetlands. Ecological Engineering 35(2), 281-289.
72. USEPA (2011) Constructed Wetlands Treatment of Municipal Wastewaters – Manual. EPA, C., USA. (ed), USEPA, https://cfpub.epa.gov/si/si_public_record_report.cfm?dirEntryId=64144.
73. Van Veen, J.A., Liljeroth, E., Lekkerkerk, L.J.A., Vandegeijn, S.C. (1991) Carbon fluxes in plant-soil systems at elevated atmospheric CO2 levels. Ecol. Appl. 1 (2), 7.
74. Wang, H., Zhao, D., Zhong, H. and Li, X. (2017) Adsorption Performance of Four Substrates in Constructed Wetlands for Nitrogen and Phosphorus Removal. Nature Environment and Pollution Technology 16（2）, 8.
75. Wang, J., Hou, J., Xia, L., Jia, Z., He, X., Li, D. and Zhou, Y. (2020) The combined effect of dissolved oxygen and COD/N on nitrogen removal and the corresponding mechanisms in intermittent aeration constructed wetlands. Biochemical Engineering Journal 153.
76. Wang Wenlin, Han Ruiming, Wan Yinjing, Liu Bo, Tang Xiaoyan, Liang Bin and Wang Guoxiang (2014) Spatio-Temporal Patterns in Rhizosphere Oxygen Profiles in the Emergent Plant Species Acorus calamus. PLoS ONE 9(5).

77. Warembourg, F.R., Roumet, C., Lafont, F. (2003) Differences in rhizosphere carbonpartitioning among plant species of different families. Plant Soil 256 (2), 11.
78. Wu, F.Y., Chung, A.K.C., Tam, N.F.Y., Wong, M.H. (2012) Root exudates of wetland plants influenced by nutrient status and types of plant cultivation. Int. J. Phytoremed. 14 (6), 11.
79. Wu, H., Fan, J., Zhang, J., Ngo, H.H., Guo, W., Hu, Z. and Lv, J. (2016) Optimization of organics and nitrogen removal in intermittently aerated vertical flow constructed wetlands: effects of aeration time and aeration rate. Int. Biodeterior. Biodegradation 113, 6.
80. Wu, H., Wang, X., He, X., Zhang, S., Liang, R. and Shen, J. (2017) Effects of root exudates on denitrifier gene abundance, community structure and activity in a micro-polluted constructed wetland. Sci Total Environ 598, 697-703.
81. Wu, S., Kuschk, P., Wiessner, A., Kastner, M., Pang, C. and Dong, R. (2013) Response of removal rates to various organic carbon and ammonium loads in laboratory-scale constructed wetlands treating artificial wastewater. Water Environ Res 85(1), 44-53.
82. Xie, X.-L., He, F., Xu, D., Dong, J.-K., Cheng, S.-P. and Wu, Z.-B. (2012) Application of large-scale integrated vertical-flow constructed wetland in Beijing Olympic forest park: design, operation and performance. Water and Environment Journal 26(1), 100-107.
83. Xu, P., Xiao, E., He, F., Xu, D., Zhang, Y., Wang, Y. and Wu, Z. (2019) High performance of integrated vertical-flow constructed wetland for polishing low C/N ratio river based on a pilot-scale study in Hangzhou, China. Environ Sci Pollut Res Int 26(22), 22431-22449.
84. Yang, L., Chang, H.-T. and Huang, M.-N.L. (2001) Nutrient removal in gravel- and soil-based wetland microcosms with and without vegetation. Ecol. Eng., 18(1), 15.
85. Zhai, X., Piwpuan, N., Arias, C.A., Headley, T. and Brix, H. (2013) Can root exudates from emergent wetland plants fuel denitrification in subsurface flow constructed wetland systems? Ecological Engineering 61, 555-563.
86. Zhang, D.Q., Tan, S.K., Gersberg, R.M., Zhu, J., Sadreddini, S. and Li, Y. (2012) Nutrient removal in tropical subsurface flow constructed wetlands under batch and continuous flow conditions. Journal of Environmental Management 96(1), 1-6.
87. Zhao, Y.J., Liu, B., Zhang, W.G., Ouyang, Y. and An, S.Q. (2010) Performance of pilot-scale vertical-flow constructed wetlands in responding to variation in influent C/N ratios of simulated urban sewage. Bioresour Technol 101(6), 1693-1700.
88. Zhu, H., Yan, B., Xu, Y., Guan, J. and Liu, S. (2014) Removal of nitrogen and COD in horizontal subsurface flow constructed wetlands under different influent C/N ratios. Ecological Engineering 63, 58-63.

964 ***Appendix: List of abbreviations***

List of symbols			
a	Parameters of the root radius, m	S_A	Fermentation products as acetate COD, mg COD L^{-3}
C_i	Concentration of the i^{th} dissolved component, mg L^{-1}	S_{ads}	Adsorbed concentration, kg kg^{-1}
Cr	O_2 concentration in the liquid phase at the root surface, kg m^{-3}	S_I	Inert soluble COD, mg COD L^{-1}
D	Mechanical dispersion, m^2 d^{-1}	S_F	Fermentable, readily biodegradable soluble COD, mg COD L^{-1}
D_{lo}	Diffusion coefficient for oxygen in the soil water, m^2 d^{-1}	S_{max}	Maximum amount of adsorbed concentration, kg kg^{-1}
IOC	Internal organic carbon load by root, mg L^{-1} d^{-1}	S_{NO}	Nitrate and nitrite nitrogen, mg N L^{-1}
k	Intrinsic permeability, m^2	S_{NH}	Ammonium and ammonia nitrogen, mg N L^{-1}
K_{grow}	Maximum growth rate of bacteria, mg L^{-1} h^{-1}	S_O	Dissolved oxygen, mg O_2 L^{-1}
K_{L}	Coefficient of Langmuir, m^3 kg^{-1}	S_o^*	Saturated dissolved oxygen, mg L^{-1}
$k_{La,A}$	Coefficient in Oxygen transmission rate of unsaturated zone, -	S_{root}^*	Interface oxygen concentration between the saturated soil layer and root surface in the liquid phase, mg L^{-1}
$k_{La,R}$	Coefficient in Oxygen transmission rate of Intermittent water supply, -		Slowly biodegradable particulate COD, mg COD L^{-1}
			Inert particulate COD, mg COD L^{-1}
		X_H	Heterotrophic bacteria, mg COD L^{-1}

$k_{La,R,dow}$	Coefficient in Oxygen transmission rate of intermitted supply in down-flow chamber, -	X_{FB}	Fermenting bacteria, mg COD L^{-1}
$k_{La,R,up}$	Coefficient in Oxygen transmission rate of intermitted supply in up-flow chamber, -	X_A	Autotrophic nitrifying bacteria, mg COD L^{-1}
κ_{rel}	Relative permeability, m^2	z	Depth, m
K_{root}	Carbon release from plants roots, mg L^{-1} h^{-1}	z_{max}	Total depth of the chamber, m
K_x	Hydrolysis rate of bacteria, mg L^{-1} h^{-1}	Z_r	Scaling depth, m
L_0	Root length density at z=0, m	α_O	Bunsen adsorption coefficient, -
m	Coefficient in van-Genuchten model, -	α	Parameter related to the air entry in van-Genuchten model, m^{-1}
$M_{\mathrm{bio_max}}$	Concentration of total microbial species which arise the microbial reproduction growth limitation, g L^{-1}	κ_{rel}	Relative permeability, m^2
M_{cap}	Concentration of total particle maters which limit the growth of microbial matters, g L^{-1}	θ	Saturation, -
n	Porosity of substrate, -	θ_{carbon}	Coefficient of calibrating K_{root} by temperature, -
OTR	Oxygen transmission rate, mg L^{-1} d^{-1}	θ_r	Residual saturation, -
p	Water pressure, Pa	θ_s	Maximum saturation, -
p_c	Capillary pressure, Pa	θ_{seff}	Effective saturation, -

q	Darcy velocity, m d^{-1}	μ	Water viscosity, kg m^{-1} s^{-1}
Q_w	Source/sink term, m^2 s^{-1}	ρ_s	Density of substrate, g cm^{-3}
R	Radius of a zone of saturated soil around the root plus the root, m	ρ_w	Water density, g cm^{-3}
ROL	Root Radial Oxygen Loss, mg L^{-1} d^{-1}	OLR	Organic loading rate, gCOD m^{-3} d^{-1}
List of abbreviations		**List of modeling cases abbreviations**	
CW	Constructed wetland	NP	Unplanted constructed wetland
IVCW	Integrated vertical constructed wetland	WP	Planted constructed wetland
DFC	Down-flow chamber of CWs	ROL	Radial Oxygen Loss only case
BOT	Bottom of CWs	IOC	Internal organic carbon loading only case
UFC	Up-flow Chamber of CWs	EOC	External organic carbon loading only case
Inf	Influent		
Eff	Effluent		